Connexin 36 Containing Gap Junctions and the Development of Blood Pressure Changes during Noxious Stimulation in Mice

by

André Coleman

A Thesis submitted to the Faculty of Graduate Studies of

The University of Manitoba

in partial fulfilment of the requirements of the degree of

MASTER OF SCIENCE

Department of Physiology of Pathophysiology

University of Manitoba

Winnipeg

Copyright © 2019 by André Coleman

Abstract

Autonomic Dysreflexia (AD) is a debilitating cardiovascular condition that often occurs after spinal cord injury (SCI). Dysregulation of the spinal sympathetic neural system predisposes individuals to life-threatening blood pressure (BP) elevations in response to noxious or innocuous stimulation. The gap junction protein connexin 36 (Cx36) has been observed in sympathetic preganglionic neurons (SPNs). Cx36 knock-out (Cx36KO) mice have decreased 24-hour BP, an attenuated pressor response to chemoreceptor activation and reduced sympatho-excitation during nociceptive stimulation. We hypothesize that Cx36KO mice have a decreased pressor response to noxious stimulation. To address our hypothesis, the carotid artery of Cx36KO and Cx36WT mice (males and females) was cannulated with a fiber optic probe. Respiratory rate (RR), heart rate (HR) and BP were measured in response to colorectal distention (CRD), electrical tail stimulation (ETS) and electrical foot stimulation (EFS). BP trended upward in Cx36WT mice during all stimulus modalities but trended downward in Cx36KO mice during CRD. We observed a trend for bradycardic response to CRD in both groups of mice but this was not a significant change. We induced a statistically significant increase in BP after intra-tracheal epinephrine injection in both groups. CRD had a much more variable effect on the RR than BP or HR. Our findings imply that non-invasive EFS may be useful for inducing AD in mice models. Contrary to our hypothesis, the pressor response in KO mice was not attenuated, but BP trended downwards during CRD. As BP increased in KO mice after epinephrine, abolition of the pressor response did not result from failure to activate peripheral adrenergic receptors, but likely an inability to activate central autonomic centers innervating the arterial vasculature. There is currently no established AD mouse model to concurrently measure BP, HR and RR responses to noxious stimulation. This work confirmed the feasibility of our mouse model for monitoring

cardiorespiratory responses to noxious stimulation. Applying our experimental design to a SCI Cx36 mouse model, the role of Cx36 in the development of AD can be investigated, which is a step towards developing more targeted therapeutic interventions.

Acknowledgements

None of my accomplishments would have been possible without blessings from the almighty. I would also like to express my deepest gratitude to my family who not only brought me into this world but provided me with the necessary guidance and support to continue living in it. Unmeasurable amounts of gratitude must be extended to my co-supervisors Drs. Katinka Stecina and Kristine Cowley. Dr. Stecina exposed me to a realm of academic mentorship that I hope all graduate students can experience. She provided tremendous lessons, advice, a positive learning environment, cake and then a little more cake. Most importantly, Dr. Stecina has surely prepared me for life after graduate school. THANKS! Dr. Cowley was always available to discuss anything, from neuroscience, to endocrinology, to theories on how life began. It was always amazing how time would suddenly vanish, as a five-minute question could become a two-hour learning activity.

Thank you to the members of my advisory committee, Drs. Brent Fedirchuk, Brian MacNeil and Brian Schmidt. I appreciated their availabilities, allowing all our meetings to occur smoothly. Thank you for the invaluable input on my project, from beginning to end. Your critiques and suggestions all helped to make this thesis what it is today.

I also want to thank our lab technician, Maria Setterbom for her expertise during the planning and execution of our experiments. She strengthened my appreciation of innovation and teamwork, skills which I will apply in many aspects of my life in the future. To Matt Ellis and Gilles Detillieux who shared their knowledge in electronics and software, I will forever be grateful. Thank you also to the administrative team: Sharon McCartney, Gail McIndless and Judith Olfert. These individuals kept me aware of events, deadlines and important university

procedures. They provided support at so many time points before and during my stay at the university.

Thank you to all my friends (you know yourselves) here in Canada, Jamaica, China and the United States who put up with my constant nagging and annoyance during the programme. I must also thank the CIHR and NSERC who funded this project. I am thankful for Dr. Todd Mondor and his generous support in the Faculty of Graduate Studies Research Completion Scholarship.

Contents

Abstract 2
Acknowledgements 4
List of Tables 8
List of Figures 9
List of key abbreviations 10
1. Introduction 11
1.1. Spinal cord anatomy 11
1.2. Epidemiology of spinal cord injury 11
1.3. Epidemiology of autonomic dysreflexia 12
1.4. Pathophysiology of autonomic dysreflexia 12
1.5. Treatment of autonomic dysreflexia 13
1.6. Review of mouse autonomic dysreflexia models 14
1.7. Spinal cord organization 15
1.7.1. Laminae of the spinal cord 15
1.7.2. Propriospinal network 17
1.8. Autonomic nervous system 19
1.8.1. Parasympathetic nervous system 19
1.8.2. Sympathetic nervous system 20
1.9. Connexins and gap junctions 21
1.9.1. Structure of connexins and gap junctions 22
1.9.2. Location of connexins in the CNS 23
1.9.3. Connexin 36 influence sensory processing 23
2. Methods 27
2.1. Spinal cord transection model 27
2.2. Arterial cannulation and cardiorespiratory monitoring during terminal experiments 29
2.3. Stimulation of afferents 30
2.4. Data analysis 32
Table 2.1. 34
Table 2.2. 35
Figure 2.1. 36
3. Results 37
3.1. BP trended upward in Cx36WT mice but downward in Cx36KO mice during CRD 37

Figure 3.1 38
3.2. Cx36KO mice and Cx36WT mice have similar HR responses to CRD 39
Figure 3.2. 40
3.3. Cx36 KO mice and Cx36WT mice have similar RR responses to CRD 41
Figure 3.3. 42
3.4. Cx36WT and Cx36KO mice have similar BP responses during EFS 43
Figure 3.4. 44
3.5. Epinephrine increases the blood pressure in both Cx36WT and Cx36KO mice. 45
Figure 3.5. 46
3.6. BP and HR responses in mice may be affected by consecutive trials of noxious stimulation . 47
Figure 3.6. 47
3.7. Electrical tail stimulation as a method for sympathoexcitation 48
Figure 3.7. 48
3.8. Experiments in spinalized animals 49
4. Discussion 50
4.1. Summary of results 50
4.2. Limitations in the methodology 51
4.2.1. Small sample size and lack of age/gender matching 51
4.2.2. Technicalities using fiber optic probe 52
Figure 4.1. 54
4.2.3. Anesthetic delivery system 55
4.2.4. Difficulties with ETS 55
4.3. The bradycardic response to CRD in isoflurane anaesthetized mice 56
4.4. Opposing blood pressure changes in Cx36WT and Cx36KO mice during CRD 58
4.5. Future directions 60
Use of gap junctional blockers in adult, spinally intact Cx36WT mice 60
The role of Cx36 in the development of cardiorespiratory changes after SCI 60
Identifying the functional role of Cx36 in cell-cell communication between SPNs 61
4.6. Summary of the potential therapeutic capacity of connexins after SCI 62
5. Conclusion 64
Table 5.1. 65
6. References 66

List of Tables

2.1. All mice used for data analysis 34

2.2. Correlation between age-BP, age-HR and age-RR responses in mice 35

5.1. Studies examining the cardiovascular responses to different stimuli in mice 65

List of Figures

2.1. Schematic illustration of experimental design and representative raw data. 36

3.1. A tendency for increased BP in Cx36WT mice but decreased BP in Cx36KO mice during CRD. 38

3.2. Cx36WT and Cx36KO mice have similar HR responses to CRD. 40

3.3. Cx36WT and Cx36KO mice have similar RR responses to CRD. 42

3.4. Cx36WT mice show a graded pressor response to electrical foot stimulation. 44

3.5. BP and HR response to intratracheal epinephrine in Cx36WT and Cx36KO mice 46

3.6. BP and HR responses decrease after consecutive trials of noxious stimulation 47

3.7. Tail stimulation increases blood pressure in Cx36WT mice. 48

4.1. Improper placement of the fiber optic probe reduces sensitivity. 54

List of key abbreviations

DBP – Diastolic blood pressure

SBP – Systolic blood pressure

HR – Heart rate

MAP – Mean arterial pressure

RR – Respiratory rate

CRD – Colorectal distention

SCI – Spinal cord injury

AD – Autonomic dysreflexia

ANS – Autonomic nervous system

SPNs – Sympathetic preganglionic neurons

Cx36 – Connexin 36

ChAT – Choline acetyltransferase

ETS – Electrical tail stimulation

EFS – Electrical foot stimulation

BP – Blood pressure

Cx36KO – Connexin 36 knock-out

Cx36WT – Connexin 36 wild-type

PN – Propriospinal neurons

NE – Norepinephrine

IML – Intermediolateral cell column

SNS – Sympathetic nervous system

PNS – Parasympathetic nervous system

LAPN – Long ascending propriospinal neurons

LDPN – Long descending propriospinal neurons

MN – Motoneurons

DA – Dopamine

CNS – Central nervous system

GABA – Gamma-aminobutyric acid

MTH – Motor threshold

1. Introduction

1.1. Spinal cord anatomy

The spinal column, also referred to as the vertebral column, forms the central axis of the skeleton in all vertebrates. The vertebral column is composed of individual bones called vertebrae, which are connected in series by ligaments and fibrocartilage (Kayalioglu, 2009). The vertebral column contains 29 vertebrae from the cranium to the sacrum in humans and 25-30 vertebrae from the cranium to the sacrum in mice (Kayalioglu, 2009, Sengul and Watson, 2012).

Enclosed within the spinal column is a near cylindrical structure which is a functional extension of the brain; the spinal cord. The mouse spinal cord contains 34 spinal segments (C_1-C_8, T_1-T_{13}, L_1-L_6, S_1-S_4 and Co_1-Co_3) while the spinal cord contains 30 neuronal segments in humans (C_1-C_8, T_1-T_{12}, L_1-L_5 and S_1-S_5) (Sengul and Watson, 2012, Frostell et al., 2016). In the adult mouse, the spinal cord terminates at the 4^{th} to 5^{th} lumbar vertebra, while it ends at the 1^{st} to 2^{nd} lumbar vertebra in humans. However, the neural and the vertebral segments are not aligned in terms of a complete overlay. Spinal roots from the lumbar and sacral segments typically emerge 4-8 vertebral bodies rostral to their segmental number in adult mice, depending on the segmental level (Frostell et al., 2016, Harrison et al., 2013).

1.2. Epidemiology of spinal cord injury

Spinal cord injury (SCI) is a life-altering and life-threatening condition affecting individuals worldwide. The estimated incidence of SCI in the United States is 17,730 new cases yearly, with an estimated prevalence of 291,000 persons (Center, 2019). In Canada, there are an estimated 4071 new cases of SCI each year (Noonan et al., 2012). The estimated incidence of SCI in Canada is 4.1 per 100,000 individuals, while the estimated incidence for non-traumatic spinal

cord disease is 6.8 per 100,000 individuals (Noonan et al., 2012). The leading cause of SCI is motor vehicle accidents (39.3%), followed closely by falls at 31.8% (Center, 2019).

Individuals with SCI have a reduced life expectancy compared to the general population. Though mortality rates due to SCI have shown a gradual decline worldwide since the 1950's, life expectancy after SCI in the United States has remained unchanged since the 1980-1990's (Center, 2019, Savic et al., 2017). The major causes of mortality include respiratory disease, infections and cardiovascular diseases (Chopra et al., 2018, Eldahan and Rabchevsky, 2018, Koseoglu et al., 2017, Savic et al., 2017).

The majority of individuals with SCI have an incomplete injury (67.5%), meaning they retain a degree of sensory and/or motor function below the level of injury. The most common injury level is cervical (C_1-C_8), resulting in 59.9% of individuals lacking sensory and/or motor functions in the lower limbs after SCI (Center, 2019).

1.3. Epidemiology of autonomic dysreflexia

Up to 92.8% of patients with chronic SCI experience paroxysmal elevations in blood pressure (BP) in response to noxious or innocuous stimuli, a condition referred to as autonomic dysreflexia (AD) (Hou and Rabchevsky, 2014, Lee and Joo, 2017). Severe BP elevations during AD can result in arrhythmia, seizures, pulmonary edema, and death (Wan and Krassioukov, 2014).

1.4. Pathophysiology of autonomic dysreflexia

Sensory afferent stimulation results in a systemic activation of the sympathetic nervous system. This is partly due to catecholamine release increases, triggered by sympathetic neurons of the

thoracolumbar spinal cord, and decreased activation of the parasympathetic outflow to the heart (Allen and Leslie, 2019). Vasoconstriction, particularly of the splanchnic vasculature, plays a major role in the regulation of circulating BP and blood volume in healthy individuals. Supraspinal autonomic centers regulate this spinal response, preventing excessive increases in BP when descending regulation of autonomic networks is intact. There is also regulation by the carotid sinus and aortic arch which stimulates the glossopharyngeal and vagal nerves to reduce the heart rate (HR) and cause vasodilation, reducing the BP. SCI below the T_6 spinal segment typically spares sufficient descending inhibition to splanchnic vasculature via supraspinal pathways, allowing adequate regulation of catecholamine-induced vasoconstriction. Lesions at or above T_6 however, prevent descending inhibition to the splanchnic vasculature during noxious or innocuous stimulation. As a result, afferent stimulation in these patients result in an exaggerated BP response from intact spinal reflexes below the level of the lesion, and a parasympathetic response with bradycardia and vasodilation above the level of the lesion (Allen and Leslie, 2019).

1.5. Treatment of autonomic dysreflexia

The mechanism underlying the exaggerated BP responses is that preganglionic sympathetic neurons, and propriospinal neurons (PN) involved in the autonomic nervous system (ANS) are dysregulated after SCI (Rabchevsky, 2006, Sharif and Hou, 2017). Current treatment regimen for AD involve a combination of pharmacological and non-pharmacological strategies. Non-pharmacological strategies include: sitting the patient upright to induce an orthostatic reduction in BP, removing offending stimuli such as constrictive clothing or a distended bladder. Pharmacological strategies include: calcium channel blockers (e.g. nifedipine) and angiotensin

converting enzyme inhibitors (e.g. captopril) with rapid onsets of action (Krassioukov et al., 2009, Squair et al., 2016).

1.6. Review of mouse autonomic dysreflexia models

According to a recent PubMed search on June 10, 2019, only six studies have investigated AD in mice. One study did not report cardiovascular changes during noxious stimulation, and all studies were performed in conscious mice, without anesthesia. A rise in blood pressure after sensory stimulation or drug administration is defined as the pressor response. The response can occur after visceral, somatic or other sensory stimulation, and is thought to reflect the increased sympathetic activity induced by the stimulus (Saha and Jayalakshmi, 2003). All experiments found in our search utilized colorectal distention (CRD) (Jacob et al., 2003, Jacob et al., 2001, Jarve et al., 2019, Ueno et al., 2016, Webb et al., 2006, Zhang et al., 2013) or cutaneous skin pinch (Jacob et al., 2003, Jacob et al., 2001, Zhang et al., 2013) as the stimulus modality. CRD was performed by inserting a balloon catheter 1 – 2 cm into the rectum and inflating it with 2 – 3 ml of air. In all mice studies identified in our search, there was an increase in BP during noxious stimulation. Lall and colleagues, however, have reported an attenuation in the pressor response to CRD in Cx36KO mice compared to Cx36WT mice (Lall et al., 2017). Only $^{3}/_{6}$ mouse papers reported changes in HR, and the direction of HR changes varied considerably in these studies. Depending on the mouse strain, the presence or absence of spinalization, there could be an increase or a decrease of the HR during CRD (Table 5). In two studies, there was a bradycardic response to noxious stimulation in spinalized mice. Another study showed a tachycardic response to noxious stimulation in spinally intact mice. However, Lall and colleagues reported a bradycardic response to noxious chemoreceptor stimulation in both Cx36WT and Cx36KO mouse preparations, concurrently with a pressor response (Lall et al., 2017). No study reported

respiratory rate (RR) changes concurrently with cardiovascular changes during noxious stimulation. Therefore, in mice, it is difficult to gauge the parameters of BP and HR shifts constituting AD, albeit it is generally accepted that it can occur on a spontaneous basis as well as induced by visceral (bowel) or somatic noxious (skin pinch) stimulation following SCI at mid-thoracic levels.

1.7. Spinal cord organization

1.7.1. Laminae of the spinal cord

The brain and the spinal cord share some similarities in neuroanatomical organization; both contain areas of myelinated axonal fibres (white matter) and regions with predominantly nerve cell bodies and dendrites (grey matter) (Brodal, 2016). Neurons in the brain can also be classified morphologically, with a fair degree of correlation between neuroanatomical structure and neuronal function (Kirkcaldie, 2012). However, the extent to which neuronal structure and function are related in the spinal cord is not fully understood. As a result, functional studies of spinal circuits are more difficult than studies in the cortex. In 1952, an important paper was published that addressed the cytoarchitectural organization of the spinal cord, significantly improving our understanding of spinal neural populations.

In 1952, Bror Rexed published a bold and challenging article after he examined the histological preparations of over 50 cat spinal cords. The techniques used by Rexed to stain thick spinal cord slices were unique compared to the use of silver impregnation or alcohol and turpentine by previous investigators (Clarke and Samuels, 1851, Clarke, 1859). Toluidine blue and gallocyanin allowed Rexed to visualize the arrangement of neural elements in the spinal cord with greater detail than his predecessors. Because of this detail, Rexed consistently delineated nine different

cellular layers in the spinal cord which he numbered laminae I-IX, based on the order of appearance dorsoventrally, and lamina X which surrounds the central canal. The overall theme of the laminae agreed with macroscopic findings, where the spinal cord could be divided into a dorsal horn (laminae I-VI) and a ventral horn (laminae VII-IX). Each lamina contains cells of varying size, shape and arrangement, with this heterogeneity further varying between lamiae (Rexed, 1952).

Lamina I contains small, medium and large sized nerve cells which are either elongated and spindle shaped; triangular or star shaped; or well rounded. Lamina II, which is split into an outer and inner layer, contains mostly small nerve cells which are either rounded or slightly elongated. Lamina III is of relatively uniform thickness with round, elongated or spindle shaped cells slightly larger than in lamina II. Lamina IV contains small, medium and large sized cells which are either rounded, triangular or star shaped. Lamina I was thought to project to the dorsal and lateral funiculi while lamina II was thought to receive small fibres from the dorsal roots**.** Laminae II-IV were believed to be involved mainly in the relay of sensory information (Rexed, 1952).

Lamina V contains cells of all sizes with small and medium cells being tightly packed medially, while larger cells are loosely packed laterally. Lamina VI is arranged in a similar fashion and both laminae were thought to be involved in intra and intersegmental motor reflexes (Rexed, 1952).

Laminae VII-IX have varying arrangements, depending on segmental location. Outside of the cervical and lumbosacral enlargements, lamina VII occupies the mediolateral extent of the intermediate zone of the cord, with laminae VIII and XI running in parallel more ventrally. At the cord enlargements, lamina VIII occupies the ventromedial aspect of the cord while lamina IX

is pushed to the ventrolateral aspect of the cord. Lamina VII increases in size and occupies even the space made between laminae VIII and IX. Lamina VII contains autonomic preganglionic cells and the sole location of the dorsal nucleus**,** while lamina VIII was thought to be involved in intra and intersegmental motor reflexes, in addition to laminae V and VI. Lamina IX was recognized to contain mainly motoneurons (MN) and formed the purely efferent layer of the grey cord matter. Lamina X has a paucity of nerve cell bodies and is the location of the dorsal and ventral grey commissures (Rexed, 1952).

Rexed's work allowed for the heterogeneity of findings by previous investigators to be combined into a single and conclusive cytoarchitectural schema. It laid the foundation for future studies into the organization of the spinal cord and manipulations of that knowledge.

1.7.2. Propriospinal network

The word propriospinal has origins from the words 'proprius' for 'one's own' and spinal. It therefore translates to mean 'belonging wholly to the spinal cord' and refers to neurons whose cell bodies and nerve terminals are both located within the spinal cord. These interneurons have been recognized as critical relays in the nervous system. Based on their location and neural connections, PN are integral in relaying descending motor commands for initiating locomotion, and information between nociceptive/noxious and spinal autonomic centers. We have started to appreciate the importance of PN, as their loss after SCI is associated with significant locomotor and autonomic dysfunctions (Rabchevsky, 2006, Cowley et al., 2010, Sharif and Hou, 2017).

PN can be differentiated based on projection (ascending/descending and ipsilateral/contralateral) and length (short axons travelling <6 segments and long axons travelling >5 segments). These

neurons are distributed throughout most spinal cord laminae and are therefore integral in relaying motor, sensory and autonomic stimuli within the cord (Conta and Stelzner, 2009).

Short axon cervical PN at the cervical enlargement are critical in modulating reaching or grasping moments in the cat, and it is believed that they serve a similar purpose in humans. A similar group of PN are in the lumbar enlargement with those projecting to proximal MN located in medial laminae VII and VIII, while those projecting to distal MN are in lateral laminae V-VII. Evidence of their role in locomotion comes from studies in which involuntary stepping was achieved in SCI patients, but only following hip extension and strong cutaneous stimulation (Conta and Stelzner, 2009). Additionally, electrical stimulation of lower limb muscles facilitates locomotor recovery in individuals with chronic SCI, possibly by activating interneuronal networks within the lumbosacral spinal cord (Angeli et al., 2018).

Long descending and long ascending PN (LDPN and LAPN respectively) connect the cervical and lumbar enlargements and are integral in forelimb-hindlimb co-ordination as well as left-right coupling, especially during activities like swimming and crawling. The LAPD however, seems to exert a stronger influence on cervical PN and not vice versa (Conta and Stelzner, 2009).

PN in lamina X modulate nociceptive, visceroreceptive and somatic input to and from the spinal cord. Their axons travel with supraspinal projections in the dorsal and dorsolateral funiculi, project to thoracic interneurons and stimulate sympathetic preganglionic neurons (Conta and Stelzner, 2009).

Choline acetyltransferase (ChAT) is an enzymatic marker for acetylcholine (ACh). Cell bodies containing ACh are found in the dorsal horn, intermediate gray and ventral horns of the spinal cord. Dorsal horn cell bodies are predominantly located in laminae III – V and serve anti-nociceptive roles. From T1 to the upper lumbar segments, ChAT positive neurons from the

intermediolateral column and intermediolateral nucleus (IML) of the spinal cord are rich in preganglionic sympathetic neurons. ChAT is also present in the MN of lamina IX, both in **α** and γ MN. There is significant dendritic bundling linking cells of similar and separate columns, possibly for synchronized and coordinated muscle activity (Heise and Kayalioglu, 2009).

Norepinephrine (NE) sensitive neurons in the dorsal horn have an anti-nociceptive effect, but more importantly, NA is involved in the relay between cardiac sympathetic and somatosensory spinal systems. NA axons from A5 terminate in lamina VII, while some axons from A7 terminate in lamina X. Stimulation of sites near the region of A5 neurons alters cardiac reflexes, and descending NA fibers may mediate the anti-nociceptive effects of acute hypertension.

DA has an inhibitory effect on spinal cord MN, as evidence by the successful use of DA agonists in treating restless leg syndrome, and dopamine receptor knock out mice have increased locomotor activity (Heise and Kayalioglu, 2009).

1.8. Autonomic nervous system

The ANS is a branch of the nervous system that regulates a broad spectrum of physiologic functions, including: BP homeostasis, bowel and bladder sphincter tone, sweating and fat metabolism. The ANS performs these functions by the coordinated activity of three major divisions; the sympathetic nervous system (SNS), the parasympathetic nervous system (PNS) and the enteric nervous system (ENS) (Wehrwein et al., 2016).

1.8.1. Parasympathetic nervous system

Parasympathetic preganglionic neurons are located either in the grey matter of the brain stem, or from the S_2 – S_4 segments of the spinal cord. Preganglionic fibres travel with either the:

glossopharyngeal, oculomotor, facial or vagal nerves. These axons synapse with postganglionic neurons in discrete autonomic ganglia, except the vagus nerve which synapses on terminal ganglia in the prevertebral plexuses (Waxman, 2017). The PNS is often referred to as the 'rest and digest' limb of the ANS. Activation of the PNS typically results in restorative or anabolic processes, such as bradycardia, increased intestinal mobility and relaxation of the urethral sphincter (McCorry, 2007). Visceral afferents from the inferior glossopharyngeal and inferior vagal nerve ganglia provide input from the heart, great vessels, respiratory and gastrointestinal tracts. These afferents are involved in reflexes that regulate BP, HR, RR and the depth of respiration (Waxman, 2017).

1.8.2. Sympathetic nervous system

Sympathetic preganglionic neurons (SPNs) have bilaterally and symmetrically located cell bodies in four spinal cord regions, from caudal C_8 to L_2-L_5. Most cell bodies are found in intermediolateral cell column (IML), located in the lateral horn of the spinal cord grey matter. The remaining cell bodies are found in the lateral funicular area, the intercalated cell group and the central autonomic nucleus (Cabot, 1990, Deuchars and Lall, 2015). The extent to which the spatial distribution of SPNs affect their function is not fully understood, but there is some evidence that SPNs on either side of the cord may have different functions. Microinjections of L-glutamate into the right IML at T_2 causes marked tachycardia and in anesthetized male Wistar rats. Similar injections into the left IML created a relatively small increase in HR, but a marked increase in contractility (Sundaram et al., 1989).

Preganglionic axons arising from the SPNs are usually myelinated and small diameter cholinergic fibres. They travel with the ventral spinal roots, forming the white rami

communicantes. Except for fibres travelling to the adrenal medulla, all preganglionic axons synapse at a postganglionic sympathetic neuron (superior sympathetic, celiac, superior mesenteric or inferior mesenteric ganglia) (Waxman, 2017).

Postganglionic axons are small, but unmyelinated adrenergic fibres. These adrenergic fibres travel with the spinal nerves to effector sites including: the gastrointestinal tract, heart, arterioles to abdominal viscera, adipose tissue, sweat glands and the lungs. Visceral afferents from pelvic and abdominal organs enter the spinal cord via thoracic, lumbar or middle sacral nerves, and can mediate activity of the ANS in response to sensory input (McCorry, 2007, Nolan et al., 1999).

The SNS is often referred to as the 'fight or flight' limb of the ANS. Activation of the SNS typically results in catabolic processes due to a massive release of NE, which then acts on target organs (such as arterioles where NE increases vasoconstriction) (McCorry, 2007, Nolan et al., 1999). One important feature of SPNs is their synchronicity, which is thought to aid in coordinating organ specific responses to systemic sympathetic activation. Indeed, previous studies have characterized the rhythmic and synchronous activity of SPNs in rats, which are features of electrically coupled neurons (Deuchars and Lall, 2015). More recently, SPNs from spinal cord recordings in neonatal mice also exhibit electrical coupling, as evidenced by the recording of spikelets when SPNs are held at -50mV during patch clamp recordings (Lall et al., 2017).

1.9. Connexins and gap junctions

Communication within and between nerves, and other non-neural cells, is essential for the conversion of electrical impulses into other useful physiological processes. The point of communication between nerves, as well as their target cells is called a synapse. Synapses can either be chemical or electrical, though some cells exhibit both. While the most common

synapses seen in the body are chemical, electrical synapses have unique and physiologically relevant properties. These properties are best appreciated when alterations in the structure or functionality of electrical synapses result in pathological conditions, or alternatively, the treatment of diseases (Dermietzel and Spray, 2016).

1.9.1. Structure of connexins and gap junctions

Gap junctions, which are the conduits through which electrical communication occurs between cells, are formed by a pair of tetraspan transmembrane connexon proteins, which are each formed by six connexin proteins. Each connexin protein has two extracellular loops, a cytoplasmic loop, an intracellular C- and N- terminal (Dermietzel and Spray, 2016, Nielsen et al., 2012). Humans, to date, are known to have a total of 21 different connexins while mice have 20 different connexins, which are numbered based on their molar masses calculated from complementary DNA (Dermietzel and Spray, 2016). The gap junctions can therefore be homo/heteromeric (based on connexins) or homo/heterotypic (based on connexons).

When two connexons from neighboring cells align, the resultant gap junction is formed with an incredibly strong hydrophobic bond, allowing the passage of molecules and ions between cytoplasms without significant leakage into the extracellular space. Flow through gap junctions can be unidirectional or bidirectional, compared to chemical synapses which only allow unidirectional flow. Connexins are selectively permeable to charge, size, or both, and distinct combinations of connexons allows selective diffusion of molecules through different cells. Through these mechanisms, gap junctions can synchronize neural activity as well as buffer various ions and metabolites between cells (Dermietzel and Spray, 2016).

1.9.2. Location of connexins in the CNS

Eleven connexin proteins have been identified within the central nervous system (Cx26, Cx29, Cx30, Cx32, Cx36/30.2, Cx43, Cx45, Cx47, Cx57, Cx59, and Cx53), which is an increase from nine connexins over the past two decades (Dermietzel and Spray, 2016, Nagy and Rash, 2000). Studies have shown gap junctional coupling between GABAergic interneurons of hippocampal and neocortical brain slices in rats (Katsumaru et al., 1988, Galarreta and Hestrin, 1999). The most abundant connexin found between neurons is connexin 36 (Cx36) and has been identified in areas such as the cerebral and piriform cortex, retina, hippocampus, thalamus, hypothalamus and mesencephalon (Dere and Zlomuzica, 2012).

Distinct connexins are identified in astrocytes or oligodendrocytes with Cx30.2, Cx32 and Cx47 being found in oligodendrocytes, while Cx30, and Cx43 are found in astrocytes (Nagy and Rash, 2000); gap junctions between astrocytes and oligodendrocytes are therefore always heterotypic (Nielsen et al., 2012). The identification of gap junctions between glial cells suggests that electrical coupling between glial cells could influence both the pathology and repair of nerve injury.

1.9.3. Connexin 36 influence sensory processing

Six decades ago, the Katz laboratory in London provided electrophysiological evidence of electrical transmission at giant motor synapses of the abdominal nerve in cray fish. As transmission occurred quickly, electrical synapses were thought to enable fast escape responses in the cray fish (Furshpan and Potter, 1959, Bennett, 1997). Four decades later, Cx36 was first identified in neurons of the mammalian brain. Using in situ hybridization, Cx36 expression has been shown in the mouse retina and brain, and neurons of the inferior olive, olfactory bulb and

hippocampus of rats (Condorelli et al., 1998, Sohl et al., 1998). Immunofluorescence studies have shown intense expression of Cx36 in laminae IV, V, VI and IX in lumbar spinal cord segments of mice, and neurons of the mesencephalic trigeminal nucleus in rats (Bautista and Nagy, 2014, Bautista et al., 2012, Curti et al., 2012).

The contribution of gap junctions to the speed of synaptic transmission in mammals has been debated previously. In colder temperatures, the speed of transmission across chemical synapses is reduced compared to electrical synapses. Cold-blooded animals therefore depend on electrical synapses to enable neuronal communication when the body temperature is decreased. However, mammalian body temperatures allow more efficient synaptic transmission across chemical synapses, which makes the contribution of electrical synapses appear redundant (Bennett, 2011, Nicholls and Purves, 1972). The question of how gap junctions influence synaptic transmission in mammals became more important after identifying the gap junction protein Cx36 at nerve terminal endings, forming anatomically mixed synapses.

Imaging studies have shown the co-localization of Cx36 and vesicular glutamate transporters (vglut) at nerve terminals in the vestibular nuclei and lumbar spinal cord, and nerve terminals in neurons of the hippocampus and trigeminal MN in rodents (Bautista et al., 2014, Nagy, 2012, Nagy et al., 2013). The working theory is that gap junctions function to promote synchronicity of neuronal discharge, both from inhibitory interneurons (e.g. in the neocortex) or projecting fibres (e.g. in the inferior olive) (Bennett and Zukin, 2004). In-vitro studies using genetically modified mice, or pharmacological manipulations have provided addition insight into the role of Cx36 in the CNS.

Cx36 knock-out (Cx36KO) mice have impairments in learning and memory (Frisch et al., 2005), a functional correlate of Cx36 expression in the hippocampus. Cx36 containing gap junctions

have been shown to be integral in sensory evoked presynaptic inhibition of large diameter sensory afferents fibers, and Cx36KO mice also have a lower seizure threshold, providing further evidence for a role of gap junctions in presynaptic inhibition (Bautista et al., 2012, Jacobson et al., 2010). Cx36 has been identified at primary afferent nerve terminals in the spinal cord which originate from large type A neurons in sensory ganglia (Bautista et al., 2014). There is also reporting of Cx36 in type B sensory neurons within lower lumbar segments, which give rise to unmyelinated fibers (Nagy et al., 2018). These reports further suggest a role for Cx36 in sensory processing. Given that functionally the presence of Cx36 results in neuro-to-neuron coupling and/or mixed electrical and chemical synapses, the processing of sensory input may differ substantially under conditions when Cx36 is a missing component of spinal synapses.

Furthermore, within the ANS, immunofluorescence studies have shown the co-expression of Cx36 and ChAT neurons in putative sympathetic preganglionic nuclei from T_6-T_8 in adult rats; nuclei in the intermediolateral cell column, intercalated group and central autonomic nucleus (Marina et al., 2008). Chemoreceptor induced excitation of the SNS was attenuated in rat working heart brainstem preparations (WHBP) after applying mefloquine, a relatively specific Cx36 gap junction blocker (Lall et al., 2012). Cx36KO mice have reduced sympathetic nerve activity and HR responses to chemoreceptor and noxious cutaneous stimulation, compared to Cx36 wild-type (Cx36WT) mice. Additionally, Cx36KO mice have a reduced HR and BP at rest compared to Cx36WT (Lall et al., 2017).

Taking all this evidence into consideration, Cx36 is located in regions of the spinal cord where neurons receive afferent input. Cx36 is present in putative sympathetic preganglionic neurons within the thoracic spinal cord. Mice lacking Cx36 have altered SNS activity, both when it develops spontaneously and when it is induced by chemoreceptor activation. We hypothesize

that mice lacking Cx36 have a reduced sympathetic response to noxious visceral stimulus, a sensory modality that has not been tested in Cx36KO mice.

In whole heart brain stem preparations of Cx36WT and Cx36KO mice, noxious chemoreceptor and nociceptive stimuli evoke both activation of the sympathetic nerves and a pressor response (Lall et al., 2017). Therefore, monitoring of the BP and the HR in vivo provides a window into the coordination between sensory and autonomic circuits. In this study our aims are to: 1) identify the role of Cx36 in the pressor response to noxious stimuli with an intact spinal cord and 2) perform a pilot study, in order to examine the contribution of Cx36 in the pathological pressor response to noxious stimuli after SCI. We **hypothesize that mice lacking Cx36 have a reduced pressor response to noxious visceral stimuli.** As the most common stimulus modalities triggering AD in humans are visceral (bladder distention and fecal impaction) (Sharif and Hou, 2017), in addition to the fact that CRD has not been tested in mice lacking Cx36, we will use CRD as our stimulus modality. Understanding what role, if any, Cx36 plays in the pressor response to noxious stimulus would provide a basis for future studies into targeted therapeutic agents for AD.

2. Methods

All experimental protocols used in this work complied with guidelines set by the Canadian Council on Animal Care. All procedures were approved by the Animal Care Committee at the University of Manitoba. Animals from two mouse colonies were used in the experiments: a B6;129S4 Gjd2tm1Paul-/-, the Cx36KO strain and a B6;129S4 Gjd2t Wt, the Cx36WT strain. Overall, 29 mice (21 – 50.2 grams) were used in these studies. Fifteen mice died before data collection.

2.1. Spinal cord transection model

Two female Cx36WT and two female Cx36KO mice were used in these experiments. Animals were given prophylactic Clavamox (50mg/kg/day) in their drinking water for three days prior to surgery. A soft (water enriched) diet was also introduced to the animals, beginning three days before surgery.

On the day of surgery, anesthesia was induced using 4% isoflurane (delivered in 95% oxygen) in a plastic box. Anesthetic depth was assessed by using the mouse's RR and the righting reflex test. The mouse was removed from the box and weighed on a digital scale. Then, the mouse was maintained on 2% isoflurane by mask so that the RR became 40 – 60 breaths per minute. Both eyes were treated with an ophthalmic ointment, and 2 mg/kg of meloxicam was administered subcutaneously. The surgical site was shaved and cleaned with chlorhexidine, 70% alcohol and 10% povidone iodine. The mouse was transferred to the surgical table and a pulse oximeter was attached to monitor HR and oxygen saturation. Isoflurane was initially maintained at 2%, but titrations were made for changes in the RR to maintain a surgical plane of anaesthesia. A heat pad was placed under the mouse to maintain a core temperature of 36 - 38℃.

Lidocaine 2% gel was applied topically to the dorsal skin and a surgical field was created using a thin layer of adhesive plastic wrap. A 1-2 cm longitudinal midline skin incision was made on the dorsal trunk, followed by blunt dissection of the ligaments and para-spinal muscles of the vertebral column. The dorsal process and vertebral bodies were removed from the vertebral bones of the third to fifth spinal segments. The overlying dura mater was incised with a small scissor, and a small amount of lidocaine 2% with epinephrine was applied over the fourth to fifth spinal segments. The T_4-T_5 spinally segment was completely transected with a 25G needle.

The injury site was washed with normal saline, and hemostasis was achieved using pressure and/or Tissue Teck adhesive. The back muscles and overlying fascia were closed using sterile absorbable 5-0 sutures. The skin incision was closed using sterile surgical clips. The animal was removed from isoflurane anesthesia and weighed on a digital scale. Buprenorphine (0.1mg/kg) and 1 ml normal saline were administered subcutaneously. The animals were then placed in their recovery cage on a heated table, where they were monitored until completely regaining consciousness.

Animals were singly housed in standard caging with soft care fresh bedding. Water and food were provided at floor level, and nutrigel was provided to animals who had difficulty eating pelleted food. Animals were monitored 2-3 times daily for the first 48 hours after surgery; looking for signs of infection, significant weight loss, intractable pain or discomfort (such as excessive grooming, aggression and decreased appetite). Bladder expression was performed every 8 hours until spontaneous bladder emptying returned. Buprenorphine 0.05 mg/kg was administered to animals displaying signs of pain or discomfort, in consultation with the Veterinary Services. Normal saline (2 mL subcutaneous) was administered every 8 hours for the

first 2 days after surgery to supplement fluid intake. External heat was also provided to the animals with warm water-filled bottles in their cages.

2.2. Arterial cannulation and cardiorespiratory monitoring during terminal experiments

Mice used in these experiments included Cx36WT and Cx36KO mice, with or without SCI. Spinalized mice were tested seven days after injury.

Anesthesia was induced with 3% isoflurane (delivered in room air) in a plastic box, after which the mouse was weighed on a digital scale. The mouse was then transferred to a heat pad and anesthesia was maintained with 2% isoflurane by mask. The mouse was placed in a supine position, and the hair on ventral midline of the neck was clipped with scissors. Lidocaine was applied topically to the ventral aspect of the neck, and a longitudinal midline skin incision was made with sharp scissors.

The connective tissue and neck muscles around the trachea were bluntly dissected using small non-toothed forceps. The left or right carotid artery was identified by its pulsatile nature and three fine threads were placed around the vessel. One upper thread and one lower thread were loosely tied and pulled in opposite directions, to lengthen and occlude the vessel as much as possible without tearing it. A second lower thread was loosely tied at the proximal end of the exposed vessel and was used to secure the fiber optic probe after cannulation. A small incision created an opening in the carotid artery and it was cannulated with the fiber-optic probe. The proximal thread was tied around the probe, securing it in the carotid artery. The tension between the upper and lower threads was then removed.

The sensitivity of the probe allowed for the monitoring of pulsatile systolic blood pressure (SBP), pulsatile diastolic blood pressure (DBP), HR and RR. These parameters were recorded by the pressure monitor (Opsense). The output was digitized, collected and stored in real time using

a custom software package designed by the Spinal Cord Research Centre (SCRC) of the University of Manitoba, Winnipeg, Canada. Mean arterial pressure (MAP) was calculated post-hoc as DBP + $^1/_3$ (SBP – DBP) by data analysis software at the Spinal Cord Research Centre.

2.3. Stimulation of afferents

In the supine position, mice were subjected to stimulation protocols aimed at activating different subsets of sensory fibres.

CRD: A latex balloon catheter (Edwards Lifesciences) was inserted 1 – 2 cm into the colorectal region. The catheter was taped to the tail and the mouse was left undisturbed for 10 – 15 minutes. Baseline data were recorded for a one-minute period, after which the balloon was inflated with air to a diameter of 4 – 5 mm. The volume of air required to distend the balloon to 4 – 5 mm was verified by always using a Luer-lock syringe for inflation. First, the inflated the balloon was measured by a ruler before inserting the catheter into the animal. Volumes of 5 mm^3 air in a 1 ml syringe, and 1.75 cm^3 air in a 3 ml syringe could consistently inflate the latex balloon to a diameter of 5 mm. The tested volume with the respective syringe and catheter was kept the same during each experiment, and removed from the animal only after all trials were completed. Distention applied at each time was typically maintained for one minute and then released completely, except in three animals when the inflated period was as indicated in Table 2. Recording continued for an additional 1-2 minutes, and then the mice were left undisturbed to allow recovering for 5-15 minutes. The distention was repeated at least once after a 5-15 minute rest period in all but one animal.

Tail Stimulation: Electrical stimulation of the tail was performed using a pair of clip electrodes (copper plated alligator clips) attached to the proximal and distal surfaces of the tail. Pulse

parameters were initially set at a frequency of 1Hz, and pulse duration of 0.2 milliseconds. The minimal intensity required to evoke a visible tail contraction was defined as the motor threshold (MTH). After identifying the MTH, the mice were left undisturbed for 1-5 minutes. Baseline cardiovascular parameters were recorded for one minute, after which electrical tail stimulation (ETS) was performed at varied intensities for 30-60 seconds, except in one animal (Table 2.). Recording continued for 2-5 minutes after the stimulus period. The mice were then left undisturbed for 3-10 minutes (a longer recovery time was given after high intensity stimulation, and a lower recovery time was given if there were no stimuli evoked changes in the measured parameters. Electrical stimulation was repeated in order to test: i) the effect of stimulation at different intensities and frequencies, and ii) changes evoked by repetitive stimuli in the same animal.

Foot Stimulation: Electrical stimulation of the foot was performed similar to as described for the tail above. The clip electrodes were placed with positive lead being above the ankle and the negative lead clipped onto the 4^{th} toe. This configuration stimulated branches of tibial nerve, including those innervating the digits. This stimulation evoked visually detectable movement of the digits. This small movement elicited by low threshold currents (0.3 – 0.5 mA) suggested a localized spread of the electrical stimulus. Stimulus intensity was graded similar to methods used for tail stimulation.

Intra-tracheal epinephrine: A stock solution of 1 mg/mL epinephrine (Sigma) was used undiluted or in a 1:10 dilution with normal saline. Variable volumes ranging from 0.01 mL to 0.05 mL were injected into the trachea.

2.4. Data analysis

The fiber-optic sensory probe was calibrated by the manufacturer so that an output of 10 mV represented 1 mmHg BP. The probe was calibrated at the beginning of each experiment by entering the calibration parameters provided by the manufacturers. The sensor's output and the digitized recordings were checked for zero baseline before cannulating the carotid artery, ensuring that zero on the sensor was also zero on the digitized signal. In five experiments, this check did not occur but the bias was minimal and equal for period before, during and after noxious stimulation. Raw wave forms were filtered (digitally) at a frequency of >3 Hz for BP measurements and 0.5 – 1.5 Hz for RR measurements. The BP, HR and RR were extracted from the wave-forms by analyzing 15 second increments before, during and after noxious stimulation. The baseline measurements were the average of the 45 – 60 second period just prior to the stimulation. The peak and the mean values (BP, HR and RR) obtained during stimulation periods were used to calculate relative changes expressed as percentage of baseline values.

Statistical comparisons of the measured values were done by using SigmaStat4.0 (Systat software, Inc., USA). The one-way ANOVA test was used to compare data from two groups (measurements from baseline vs. stimulation and peak percent changes between KO and WT). The steps used by the program consisted the following steps: the Shapiro-Wilk test was used to check for normality and there was a normal distribution in each set of samples. Then the Brown-Forsythe test was used as the Equal Variance Test. When passed, the difference between the group mean values was compared. If there was a greater than would be expected by chance; pairwise multiple comparison procedures of the Tukey Test was used. Lastly, the power of performed test with alpha = 0.05 was also reported. Measurements for mean percent changes

between KO and WT were analyzed using two sample t-tests using the data analysis pack in Microsoft Excel 2016.

Table 2.1. All mice used for data analysis.

Experiment number	WT/KO	Sex	Age (days)	Weight (g)	CRD	ETS	EFS	Epinephrine
6[1, 5]	KO	M	239	37.2	x2	x5	-	-
27	KO	M	99	26.6	x4	x3	x13	0.04mL-0.1mg/mL
12[2]	KO	F	298	32.6	x2	-	-	-
13	KO	F	213	28	x3	x3	-	-
15	KO	F	240	21	x2	x3	-	0.01mL-1mg/mL
16[4]	KO	M	244	34.4	x1	-	-	-
17	KO	M	245	31.8	-	-	x13	0.01mL-1mg/mL
19	KO	M	253	42.5	-	x1	x12	0.05mL-0.1mg/mL
20	WT	M	98	31.1	-	-	x9	0.03mL-0.1mg/mL
21[6]	WT	M	99	32.5	x7	-	x14	0.05mL-0.1mg/mL
23	WT	F	103	26.1	x8	x5	x6	0.03mL-0.1mg/mL
24	WT	F	104	29.8	x2	x3	x14	0.01mL-1mg/mL
25[3]	WT	M	105	30.2	x6	x7	x14	0.03mL-0.1mg/mL
11	WT	F	272	33.6	x5	x8	x5	-

The columns indicate the experiment number; the mouse colony examined: Cx36WT (WT) or Cx36KO (KO); the sex of the mouse: male (M) or female (F); the age of the mouse in days; the weight of the mouse in grams; the number of times each stimulus modality was applied ('-' = none); the volume and concentration of epinephrine administered ('-' = none); [1] Only RR analyzed; [2] Only RR and HR analyzed; [3] CRD maintained for 48 seconds; [4] CRD maintained for 20 seconds; [5] CRD maintained for 69 seconds; [6] EFS maintained for 75 seconds

Table 2.2. Correlation between age-BP, age-HR and age-RR responses in mice

Correlation values	WT	KO
CRD induced BP change vs. age	0.43	-0.09
CRD induced HR change vs. age	0.65	-0.11
CRD induced RR change vs. age	0.41	-0.21

The columns indicate the variables examined for correlation; the correlation coefficients for measurements in Cx36WT mice (WT); and in the Cx36KO mice (KO).

Figure 2.1.

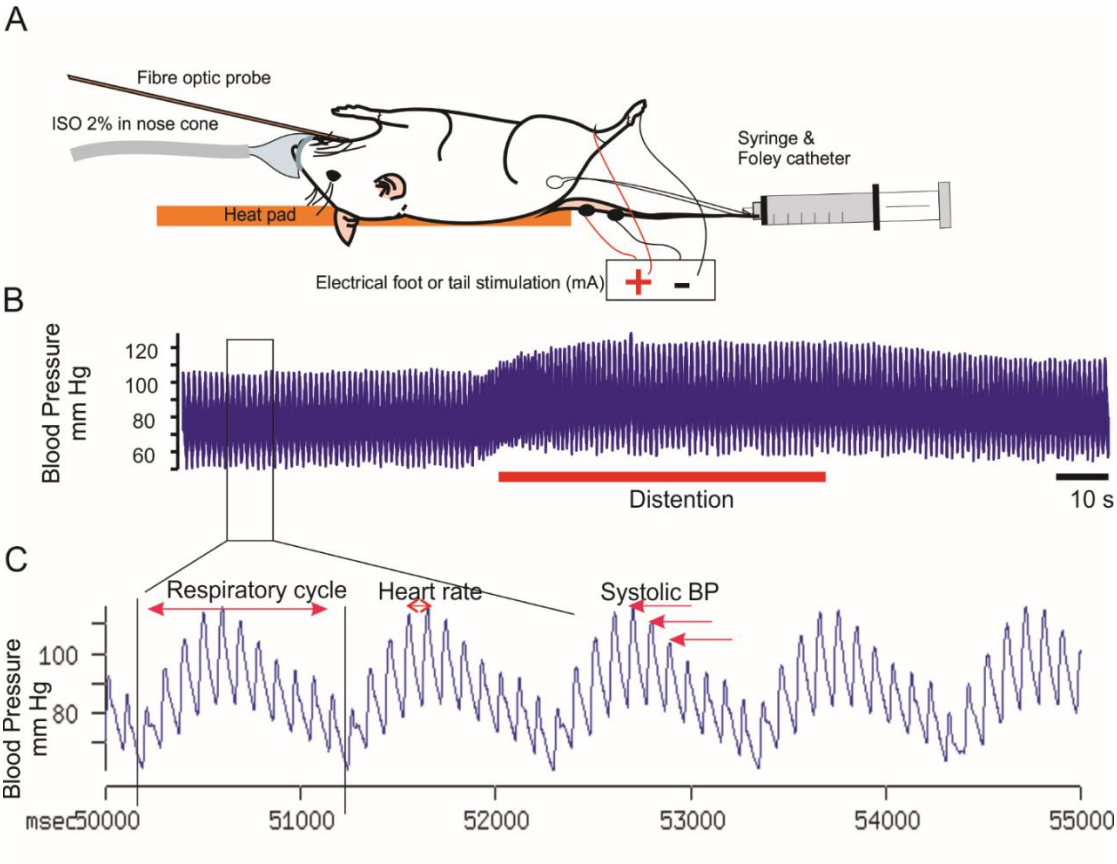


Fig. 2.1. Schematic illustration of experimental design and representative raw data.

A. Mice were anaesthetized with vaporized isoflurane in room air (3% for induction and 1.8-2.3% for maintenance). A fiber optic probe inserted into the carotid artery collected MAP, SBP, DBP, HR and RR in real time. Changes in parameters were collected in response to CRD, EFS and ETS. CRD was performed by inflating a latex balloon catheter to a diameter of 4 – 5 mm. Electrical stimulation of the tail and foot were performed at intensities of 1 – 100x MTH at frequencies of 1 or 4 Hz. **B.** Raw wave form from a representative Cx36WT mouse (272 day old male). The fiber optic probe records real time changes in BP before, during and after noxious stimulation. **C.** Raw wave form from B at a higher magnification. The data from the fiber optic probe can be analyzed to measure the HR, respiratory cycle, SBP and DBP. MAP was calculated post-hoc using the SBP and DBP.

3. Results

3.1. BP trended upward in Cx36WT mice but downward in Cx36KO mice during CRD

We measured BP in both WT and KO mice before, during and after CRD. We observed that Cx36WT mice had a tendency for an increase in BP during CRD, which peaked at 30 – 45 seconds after initiating CRD (Fig 3.1A). All but one Cx36WT mouse showed this tendency for an increase in BP during CRD when we used the trial with the maximum change (Fig 3.1B). On the other hand, all Cx36KO mice had a tendency for a decrease in BP during CRD, reaching a nadir at 15-30 seconds of distention (Fig 3.1A, C). However, the BP increase in the Cx36WT and the decrease in the Cx36KO mice was statistically insignificant.

We calculated the BP change during CRD using the mean change in the stimulus period, as well as the peak change during the stimulus period. The mean SBP in the Cx36WT group trended upwards from a baseline of 92.7 ± 9 mmHg to a peak of 104.3 ± 24 mmHg during CRD (n = 5). The mean SBP in the Cx36KO group trended downwards from a baseline of 94.0 ± 19 mmHg to a nadir of 88.3 ± 21 mmHg during CRD (n = 4,). However, these trends did not reach statistically significant levels (p = 0.36 and p = 0.70 for the increase and the decrease, respectively, by ANOVA test).

We also compared the relative changes (percentage of baseline) in parameters measured. The percentage mean changes in BP were 7.3 ± 15% and -2.8 ± 2% in Cx36WT and Cx36KO mice respectively (p = 0.22). The percentage peak changes in BP were 11.8 ± 20% and -6.4 ± 6% in Cx36WT and Cx36KO mice respectively (p = 0.13) (Fig 3.1D). Though there was a trend for percentage peak changes in BP to be larger than percentage mean changes in both groups of mice, this did not reach statistical significance (p = 0.70 for WT; p = 0.31 for KO) (Fig 3.1D).

Figure 3.1

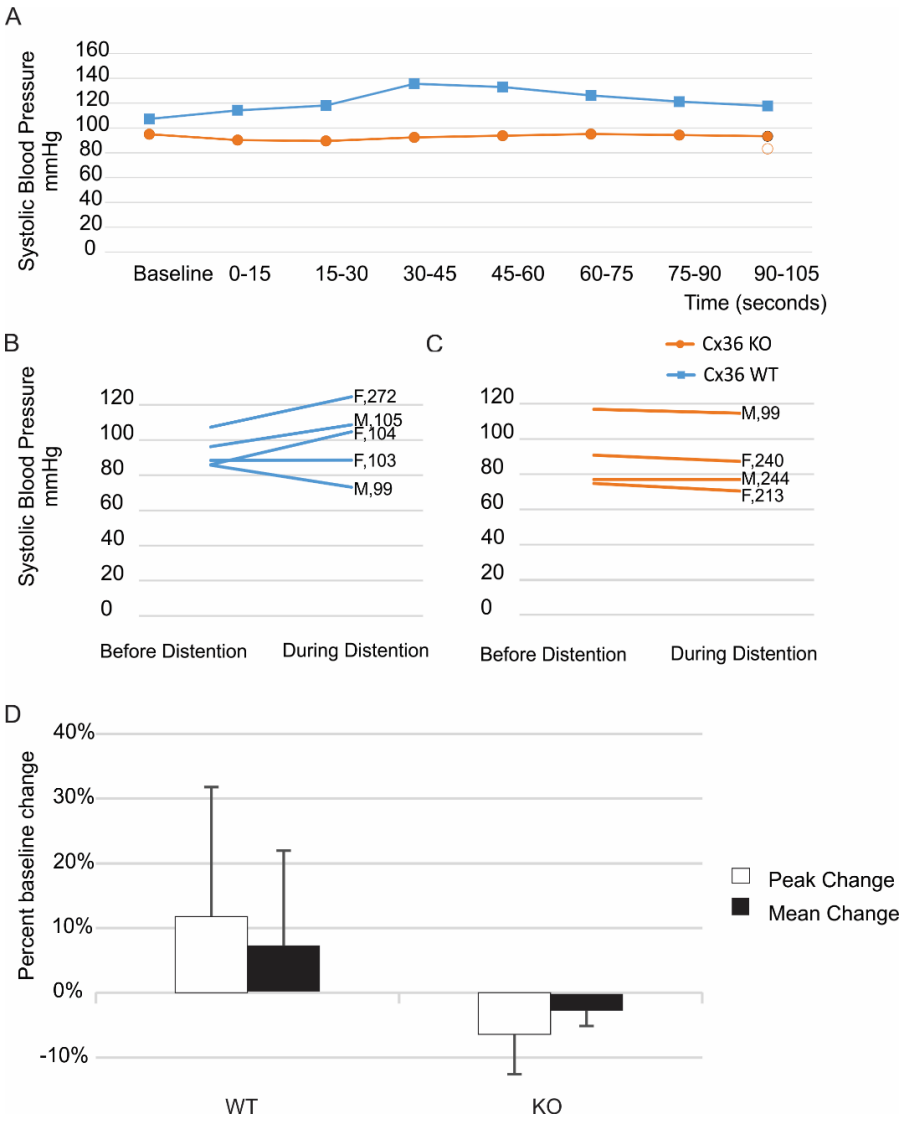


Fig 3.1. A tendency for increased BP in Cx36WT mice but decreased BP in Cx36KO mice during CRD

A. Mice [Cx36WT (272 days) and Cx36KO (240 days)] exposed to 1 minute of CRD show a transient BP change during CRD. **B.** All data from WT (n = 5) showing mean BP before and during distention. **C.** All data from KO (n = 4) mice showing mean BP before and during distention. **D.** Changes in BP were calculated using the peak and average BP recorded during CRD expressed as a percentage of baseline BP. Data presented as mean ± S.D.

3.2. Cx36KO mice and Cx36WT mice have similar HR responses to CRD

Concurrently with BP monitoring in our mice, we measured HR changes during CRD. HR reached a nadir after 45 – 60 seconds of CRD and began recovering almost immediately after deflation of the balloon catheter in Cx36WT mice. Cx36KO appeared to have a delayed HR recovery after CRD (representative data from a 272 day old WT and a 240 day old KO shown in Fig 3.2A).

As illustrated in Fig 3.2, the HR before stimulation was within a wider range in the Cx36KO mice (Fig 3.2B) than in the Cx36WT mice (Fig 3.2C). However, this did not seem to influence the overall reduction in HR during CRD. Mean HR trended downwards from a baseline of 591.4 ± 22 beats/min to a nadir of 573.6 ± 21 beats/min in Cx36WT mice (n = 5, $p = 0.23$). There was also a downward trend for mean HR in Cx36KO mice, from a baseline of 586.3 ± 69 beats/min to a nadir of 577.7 ± 77 beats/min (n = 5, $p = 0.86$).

The percentage mean changes in HR were -2.0 ± 1% and -0.8 ± 1% in Cx36WT and Cx36KO mice respectively. ($p = 0.10$) Peak HR during CRD expressed as percentage of baseline was -3.0 ± 1% and -1.6 ± 2% in Cx36WT and Cx36KO mice respectively ($p = 0.23$) (Fig 3.2D). The percentage mean and percentage peak changes in HR were also similar within mice groups ($p = 0.12$ for Cx36WT; $p = 0.48$ for Cx36KO) (Fig 3.2D).

Figure 3.2.

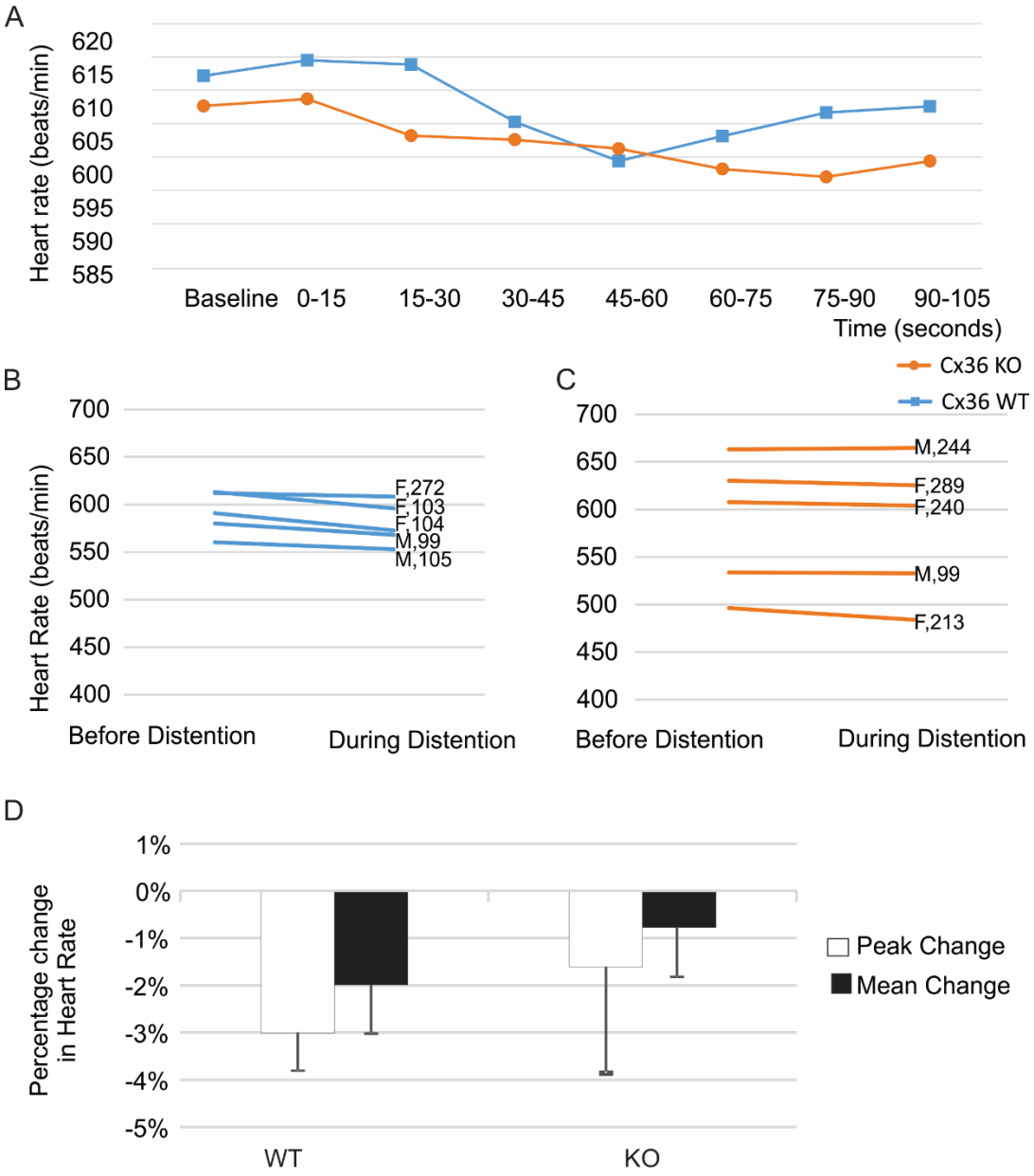


Fig 3.2. Cx36WT and Cx36KO mice have similar HR responses to CRD.

A. The same mice as in Fig 5.1A, show a downward trend for HR during CRD. **B.** All data from WT (n = 5) showing absolute HR values before and during CRD. **C.** All data from KO (n = 5) mice showing mean HR before and during CRD. **D.** Changes in HR calculated using the peak and average HR recorded during CRD expressed as a percentage of baseline HR. Data presented as mean ± S.D.

3.3. Cx36 KO mice and Cx36WT mice have similar RR responses to CRD

In addition to BP and HR, we also monitored mice for changes in their RR during CRD. We observed that both Cx36WT and Cx36KO mice had an increased respiratory during CRD (representative data from a 272 day old WT and a 239 day old KO mouse shown in Fig 3.3A). The RR reaches a peak level after 15 – 45 seconds of CRD (Fig 3.3A).

As illustrated in Fig 3.3B, the direction of change in RR in response to CRD was more variable in WT mice, with the RR trending downward in $^{2}/_{5}$ WT mice, (Fig 3.3C) while the RR trended downward in $^{1}/_{6}$ KO mouse (Fig 3.3B). The mean RR trended upward from a baseline of 61.4 ± 14 breaths/min to a peak of 69.6 ± 22 breaths/min in Cx36WT mice (n = 5, p = 0.51). In Cx36KO mice, the mean RR trended upward from a baseline of 50.0 ± 11 breaths/min to a peak of 59.1 ± 13 breaths/min (n = 6, p = 0.22).

The percentage mean change in RR from baseline was 7.4 ± 17% and 6.1 ± 17% in Cx36WT and Cx36KO mice respectively (p = 0.90). Peak RR expressed as percentage of baseline was 15.5 ± 34% and 21.8 ± 28% in Cx36WT and Cx36KO mice respectively during CRD (p = 0.75) (Fig 3.3D). The percentage mean and percentage peak changes in RR were also similar within mice groups (p = 0.65 for Cx36WT; p = 0.27 for Cx36KO) (Fig 3.3D).

Figure 3.3.

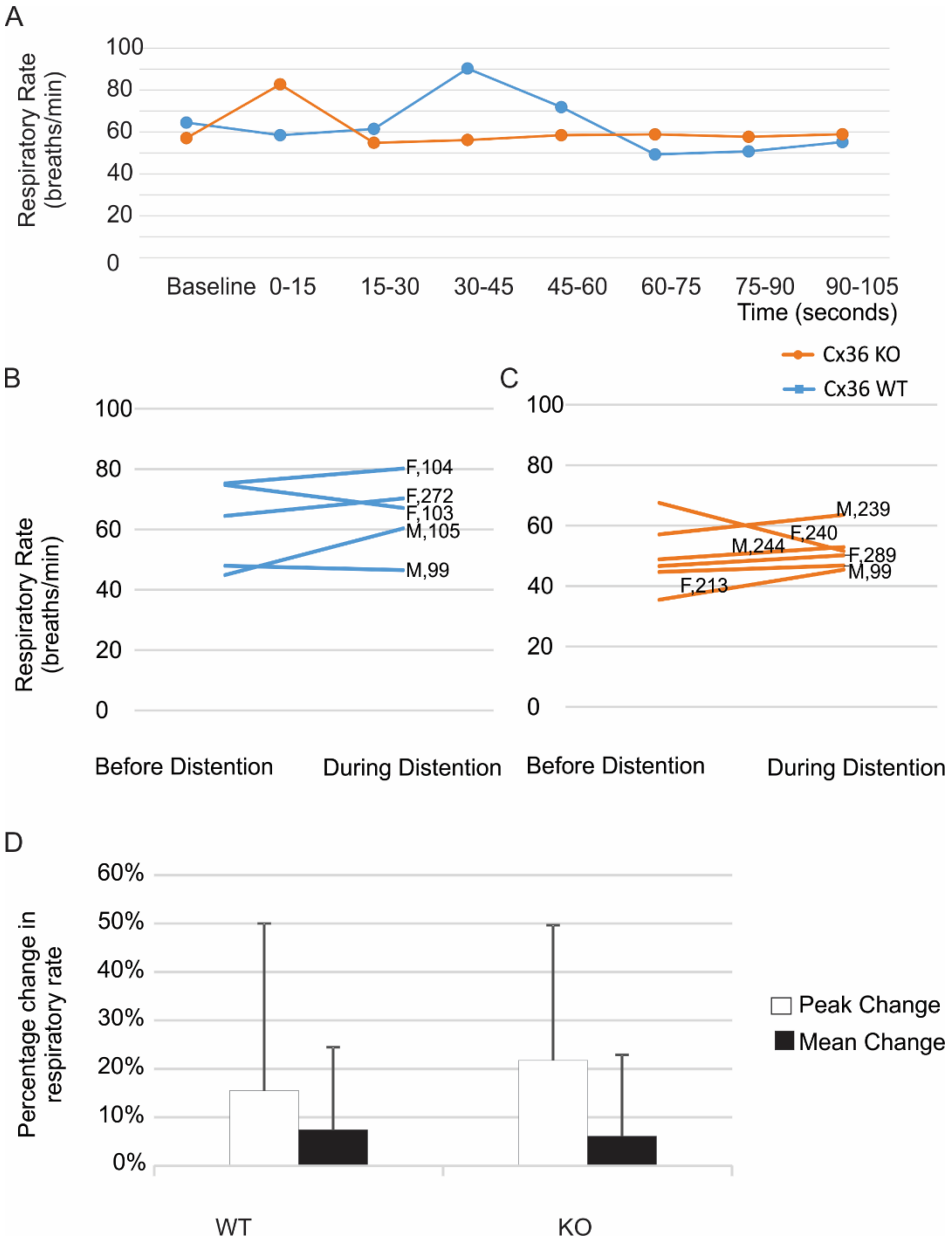


Fig 3.3. Cx36WT and Cx36KO mice have similar RR responses to CRD.

A. Mice [WT (272 days old) and KO (239 days old)] showed an upward trend in RR during CRD. **B.** All data from WT mice (n = 5) showing mean absolute RR before and during CRD. **C.** All data from KO mice (n = 6) showing mean RR before and during CRD. **D.** Changes in RR calculated using the peak and average RR recorded during CRD expressed as a percentage of baseline RR. Data presented as mean ± S.D.

3.4. Cx36WT and Cx36KO mice have similar BP responses during EFS

To investigate the effect of electrical stimulation of the foot on BP, WT and KO mice were subjected to 1 Hz or 4 Hz electrical shocks at varied intensities. Representative data from a 105 day old Cx36WT mouse subjected to EFS at a frequency of 4Hz, and intensities of 3 – 15x motor threshold (MTH) is shown in Fig 3.4A-E. There was an increase in the pressor response with higher intensities of electrical shock. Similar responses were obtained from $^{5}/_{6}$ WT mice and $^{2}/_{4}$ KO mice (Table 2.).

Selecting those trials in which the smallest intensity stimulation evoked distinct visually recognizable BP increases (n = 5 WT; n = 2 KO), we found a consistent upward trend in averaged absolute BP during EFS (Fig 3.4F, G). These changes were small as a percentage of baseline BP (3.03 ± 0.9% in Cx36WT and 2.57 ± 2% in Cx36KO mice) , but consistent between the two mice lines (p = 0.63) (Fig 3.4H).

Figure 3.4.

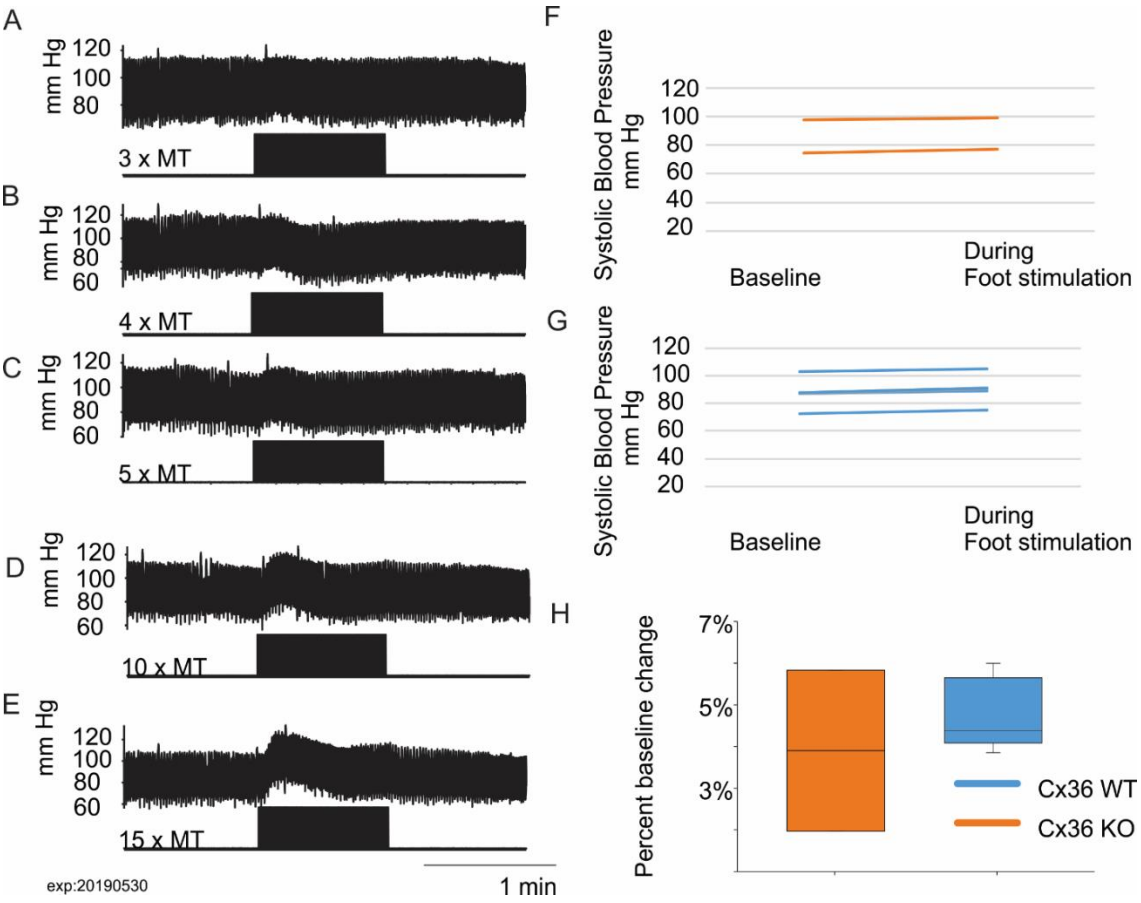


Fig 3.4. Cx36WT mice show a graded pressor response to electrical foot stimulation.

Representative data from a Cx36WT mouse subjected to EFS at a frequency of 4Hz, and intensities of 3x MTH **(A)**, 4x MTH **(B)**, 5x MTH **(C)**, 10x MTH **(D)** and 15x MTH **(E)**. There was an increase in the pressor response with higher intensities of electrical shock. **F**. All data from Cx36KO mice (n = 2) showing mean BP before and during 4 Hz EFS (2x and 4x MTH). **G**. All data from Cx36WT mice (n = 5) showing mean BP before and during 4 Hz EFS (1x – 10x MTH). **H**. Changes in BP calculated using the average BP recorded during EFS expressed as a percentage of baseline BP. The mean (solid line) the 10th and 90th percentiles (error bars) and 25th and 75th percentile (box) values are indicated for KO mice. The mean (solid line) and range (box) are indicated for WT mice.

3.5. Epinephrine increases the blood pressure in both Cx36WT and Cx36KO mice.

In order to investigate the role of Cx36 in the sympathetic driven BP increase after epinephrine, mice were given intra-tracheal injections of 0.01 – 0.05 mL of a 0.1 mg/mL solution of epinephrine. Cx36WT and Cx36KO mice had an increase in mean absolute BP after administration of epinephrine (Fig 3.5A, B). Except for one WT mouse (Fig 3.5B), all mice showed an increase in BP after epinephrine injection. This was a statistically significant increase from a baseline of 79.9 ± 9 mmHg to a peak of 99.8 ± 11 mmHg in the WT animals (n = 4, p = 0.04). The baseline BP of 66.9 ± 18 mmHg increased to a peak of 158.0 ± 58 in the KO mice (n = 4, p = 0.01). The increase in mean absolute BP, expressed as a percentage of baseline BP was seemingly larger in KO mice (Fig 3.5C). However, the volume of drug administered was greater in some KO mice that the volume given to the WT animals (Table 2.), therefore comparisons between results from the two lines were not made in this case.

Concurrently with the BP, we also analyzed the HR before and after epinephrine administration in the same mice. Cx36KO mice (n = 4) had a consistent decrease in HR after epinephrine (Fig 3.5D). However, after epinephrine administration in Cx36WT mice, the HR increased in $^{3}/_{4}$ experiments (Fig 3.5E).

Figure 3.5.

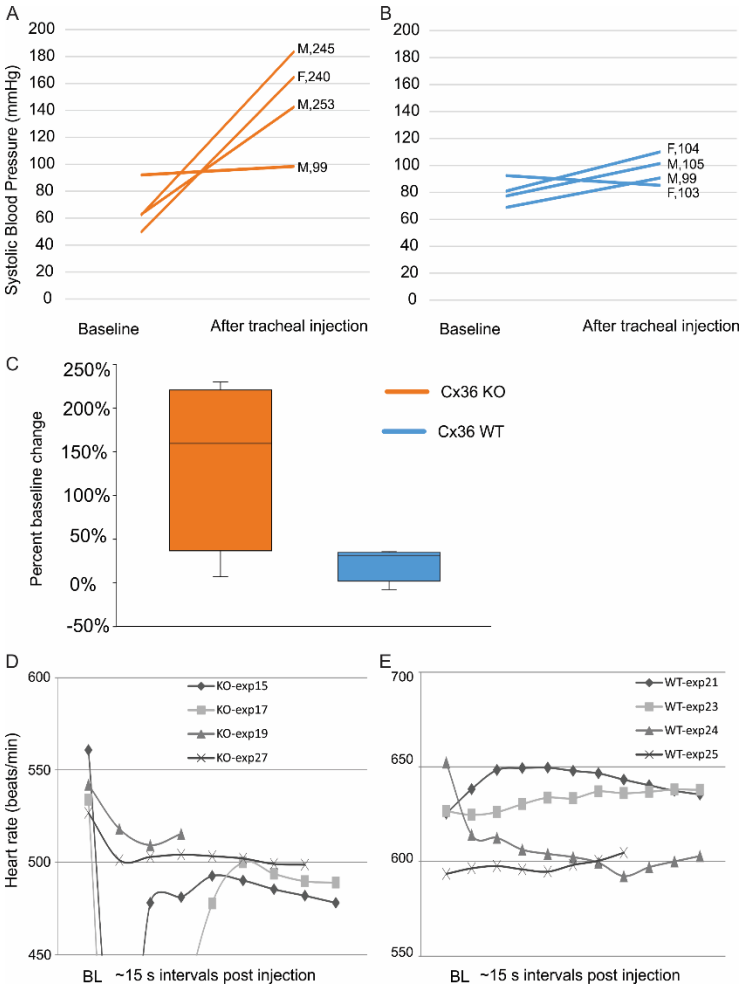


Fig 3.5. BP and HR responses to intratracheal epinephrine Cx36WT and Cx36KO mice.

A. All data from Cx36KO mice (n = 4) showing mean BP before and after intra-tracheal injection of epinephrine. **B.** All data from Cx36WT mice (n = 4) showing mean BP before and after intra-tracheal injection of epinephrine. **C.** Changes in BP calculated using the average BP recorded after EFS expressed as a percentage of baseline BP. The mean (solid line) the 10th and 90th percentile (error bars) and 25th and 75th percentile (box) values are indicated. **D.** Mean HR at baseline and during 15 second intervals after epinephrine in Cx36KO mice. **E.** Mean HR at baseline and during 15 second intervals after epinephrine in Cx36WT mice. BL – Baseline

3.6. BP and HR responses in mice may be affected by consecutive trials of noxious stimulation

In order to investigate how repetitive episodes of noxious stimulus might affect the magnitude of the cardiorespiratory response, mice were subjected to consecutive trials of CRD. BP and HR were monitored and analyzed during CRD as described in the methods. We observed that the magnitude of change in both the BP (Fig 3.6A) and HR (Fig 3.6B) during CRD was decreased in the second trial compared to the initial trial (data from 272 day old WT mouse). Percentage peak MAP during CRD decreased from 21.9% in trial 1 to 12.4% in trial 2. We observed a similar trend in Cx36WT and Cx36KO mice exposed to consecutive trials of noxious stimulation (Table 2.).

Figure 3.6.

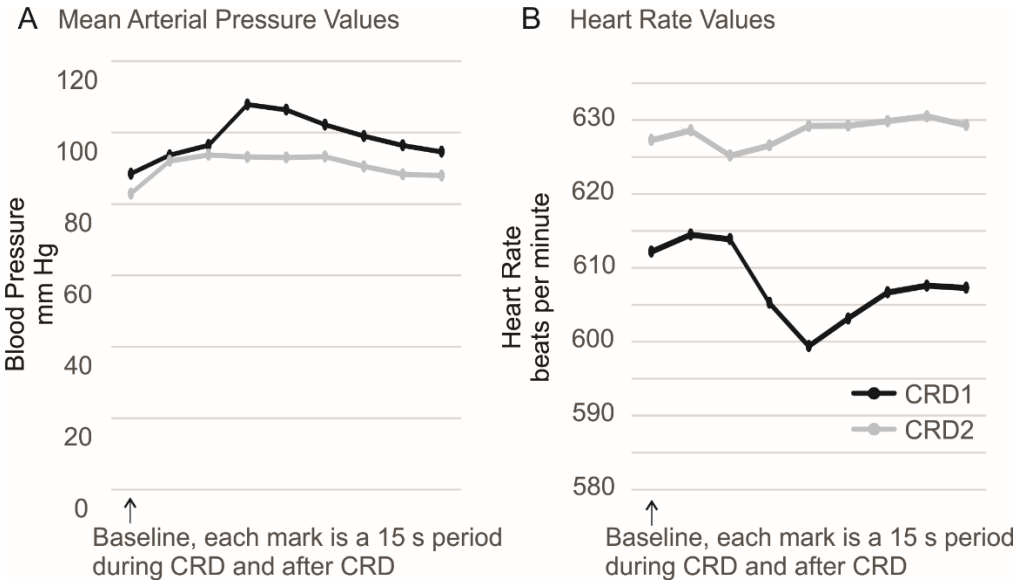


Fig 3.6. BP and HR responses are not identical after consecutive trials of noxious stimulation in mice.

Cx36WT mouse showing a change in the cardiovascular response to noxious stimulation after consecutive trials. **A.** The upward trend in BP seen in CRD trial 1 is attenuated in CRD trial 2. **B.** The downward trend HR observed in CRD trial 1 is attenuated in CRD trial 2.

3.7. Electrical tail stimulation as a method for sympathoexcitation

To investigate the effect of electrical stimulation of the tail on BP, WT and KO mice were subjected to 1 Hz or 4 Hz electrical shocks at varied intensities. Representative data from a 103 day old Cx36WT mouse is shown in Fig 3.7. Tail stimulation at a frequency of 4 Hz evokes a BP increase, which we observed in $^{3}/_{8}$ experiments.

Figure 3.7.

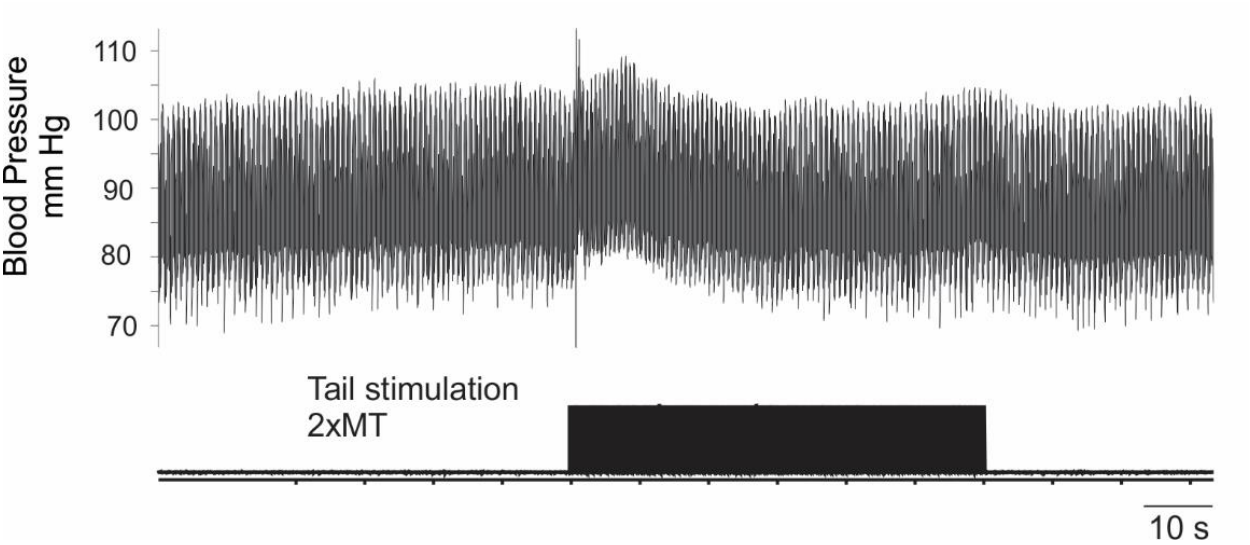


Fig 3.7. Tail stimulation increases blood pressure in Cx36WT mice.

Representative data from a Cx36WT mouse subjected to 4 Hz ETS at 2x MTH. A transient BP increase is seen after starting stimulation. BP returns to baseline after ~20 seconds of stimulation.

3.8. Experiments in spinalized animals

In order to test the cardiovascular response of spinalized Cx36WT and Cx36KO mice to noxious stimulation, two WT and two KO mice were subjected to a complete spinal cord transection (SCT) and $T_4 – T_5$. One mouse died as due to an immediate complication during the spinalization surgery. One mouse was lost on the third recovery day after complete SCT. One mouse died while cannulating the carotid artery when performing the terminal experiment to test autonomic dysreflexia. One mouse survived arterial cannulation for terminal experiments but had an incomplete SCT as evidenced by preserved hindlimb locomotion and we were unable to collect data on BP during CRD. These preliminary spinalization series have shown that mice lose significant mobility and have impaired temperature regulation after complete SCT at $T_4 – T_5$.

4. Discussion

4.1. Summary of results

Our experiments are the first to simultaneously examine the cardiac and respiratory changes following CRD in isoflurane anesthetized mice. Cx36WT mice showed a tendency for BP to increase during CRD, while Cx36KO mice showed a downward trend in BP during CRD. However, no significant differences were detected between BP measurements obtained at baseline and during CRD. We have also found that CRD has a much more variable effect on the RR than BP or HR. Another interesting finding was that the HR trended downwards in both mice lines during CRD. We also obtained preliminary data showing that CRD induced smaller cardiovascular responses in consecutive trials of noxious stimulation.

Our study is the first to examine the cardiorespiratory response to electrical stimulation of the foot. There was a graded increase in BP during 4Hz EFS in both Cx36WT and Cx36KO mice when using intensities within 2-30 times the intensity required to excite the motor response in the digits. Our sample size was too small for statistical comparisons, however, with these experiments, we established a stimulation protocol and a common pattern, verifying that the 4 Hz stimulation rate does induce sympatho-excitation, similar to what has been described in rats in terms of neurogenic pain (Gonzalez et al., 2005)

Lastly, this study has attempted to test AD responses in spinalized animals, however, no quantitative data was obtained from the batch of mice after high-thoracic spinalization. These experiments as pilot trials established some key postoperative interventions that are necessary for the success of future experiments. For example, the need of heated cages, regular saline injections for hydration and regular bladder expressions are all equally critical for the optimal

survival of these mice to the desired time point after spinal cord injury (about 7-9 days post spinal cord injury).

In summary, the key results include the optimization of the pressor response testing procedures in mice. It is important to highlight that none of these methods have been used in the laboratory before I started my training. Therefore, the refinement of the approaches used for a) long-term BP monitoring in mice while applying stimulation of visceral and hindlimb afferents and b) development of procedures and post-operative care after high spinal cord lesions in mice have been crucial aspects of my contribution in this project. In terms of the directional difference in the BP response identified between Cx36WT and Cx36KO mice, more experiments will be necessary to verify whether differences between the baseline and stimulation conditions are statistically different or not.

4.2. Limitations in the methodology

4.2.1. Small sample size and lack of age/gender matching

Our sample size was small and except for one pair of WT and KO mice, the animals were not matched for age and gender (Table 2.). The average ages were 228.88 ± 57.56 days and 130.17 ± 69.54 days for Cx36KO and Cx36WT mice respectively. In-vivo experiments performed by Lall et al. 2017, used only female Cx36WT or Cx36KO mice aged 6 – 8 months. Previous literature has documented changes in developmental expression of Cx36 within the spinal cord of mice (Bautista et al., 2014), but there is also evidence of Cx36 co-expression in the IML of adult mice (Lall et al., 2017).

Mice used in this study were generated using a global, rather than a conditional deletion of Cx36. In addition to deficits in learning, memory, and cardiovascular function, the existing literature

also suggests a role for Cx36 in the development of tactile allodynia. Mice subjected to intrathecal injections of small interfering RNA had decreased expressions of Cx36 in the dorsal horn of the lumbar spinal cord, and developed tactile allodynia of the hind paws (Nakamura et al., 2015). This finding also relates to the identification of Cx36 containing gap junctions at inhibitory GABAergic interneurons (Bautista et al., 2014, Bautista et al., 2012).

Furthermore, in the same knock-out strain we used, a reduction in the amplitude of spontaneous contraction within colonic smooth muscle was described recently – however, colonic muscle strips from these mice also have increased responsiveness to cholinergic stimulation (Nagy et al., 2014).

4.2.2. Technicalities using fiber optic probe

In Table 2. and in the results, we reported data from fourteen experiments, however, we performed an additional set of terminal experiments on spinalized and spinally intact mice (n = 2 and n = 11 respectively) in the early phase of this project. We attempted to use a fluid-filled cannula interfacing the blood in the carotid to measure the BP in eight of these experiments. The most common method of arterial cannulation in mice studies assessing AD was polyethylene tubing (PE) (Jacob et al., 2001, Jarve et al., 2019), and one study used radiotelemetry (Zhang et al., 2013). Based on the literature, we also attempted to use polyethylene tubing (PE-8, PE-10 sizing) in our experiments. Six mice died due to excessive bleeding after PE cannulation. The lumen of the carotid artery in mice has a small diameter, which was difficult to cannulate safely with even the small size PE-8 tubing. Furthermore, when arterial cannulation was successful, we noted deterioration of the BP signal, possibly due to coagulation and occlusion of the small cannula. We therefore opted to use a fiber optic probe that converts mechanical-based sensations to an electrical signal. The insertion of the FO cannula was also difficult initially, with a total of

five mice dying due to excessive bleeding after FO cannulation. Nonetheless, our cannulation success increased over the course of these experiments. Importantly, this instrument is so sensitive that it records the waves created by the systolic and diastolic BP fluctuations, and the fluctuations due to the RR. Working with this method, albeit, also has some limitations that are discussed below.

The positioning of the probe relative to the mouse's body has been a source of error. We tried to be consistent in the orientation of the probe, its angle of entry into the carotid artery and the distance from the chest and stomach. In one experiment, the digitized waveform from our fiber optic probe did not display all the heart beats in each respiratory cycle (Fig 4.1A). After the fiber optic probe was repositioned more distally in the carotid artery, the digitized waveform displayed all expected heart beats in a respiratory cycle. Additionally, when the position of the probe was sub-optimal, the BP response to CRD was also affected (Fig 4.1B). Essentially, the pressure signal from the HR could be attenuated by either tension in the probe or by mechanical pressure on the probe by surrounding organs/structures. The working protocol that we developed based on the observed limitations include: 1) the zero-position check immediately prior to insertion and 2) the validation of the recorded waveform immediately after the insertion of the probe. If there is attenuation of individual heart beats, then re-alignment of the probe is attempted to reduce the error.

Figure 4.1.

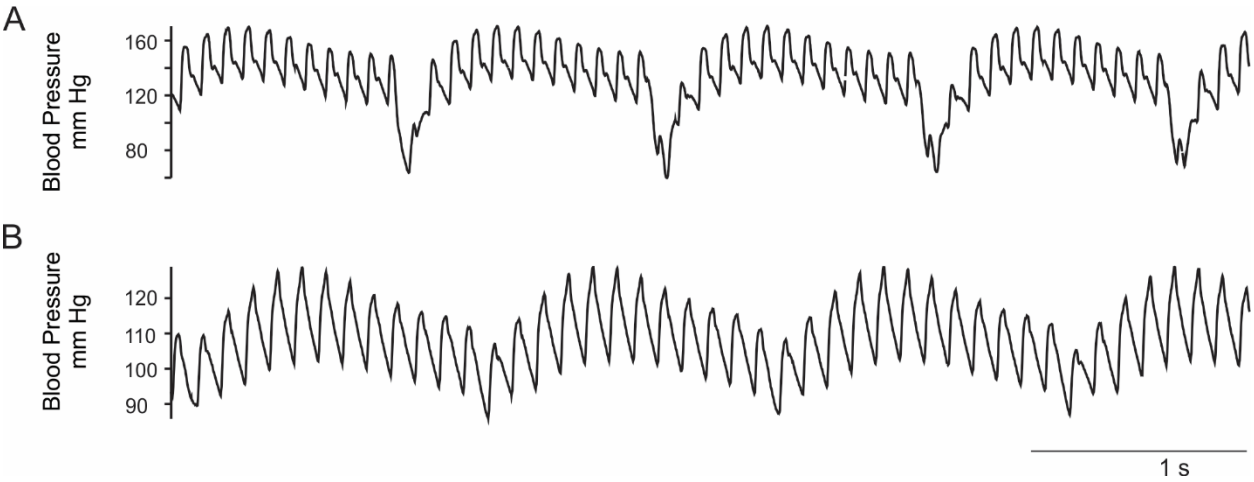


Fig 4.1. Improper placement of the fiber optic probe reduces sensitivity.

Data from a 99-day old Cx36KO mouse. **A.** Digitized waveform during a baseline period shows attenuation of ~2 heart beats per respiratory cycle. There is also a reduction in the variability of the SBP and DBP during respiration. The absolute values for the SBP and DBP are also elevated. **B.** After repositioning the fiber optic probe, there is normalization of the waveform, with the recording of each heartbeat without distortions during the respiratory cycles. The SBP and DBP have returned to lower values and regained the expected variation during respiration.

4.2.3. Anesthetic delivery system

We have used a recently developed small animal anesthesia system, the SomnoSuite delivery system for these studies. This system is based on small (low-volume, 30-50 mL/min) gas flow to the animal and the anesthesia delivered can be titrated with concentrations of anesthesia in increments of 0.1% (delivered in room air during these experiments). The mice were anesthetized with a mask that did not create an air-tight enclosed gas delivery system. As such, the dead space between the delivery system and the alveoli of the mice was unmeasurable and unpredictable. This led to a discrepancy in the concentration/volume of anesthesia being delivered by the system, and the actual concentration/volume of anesthesia inhaled by the mice. We attempted to mitigate this problem by using the HR and RR to assess the depth of anesthesia, but we cannot rule out the possibility of inadvertently over-anesthetizing mice in some experiments. It is known that the concentration of isoflurane being delivered to C57BL/6 mice can affect their HR and BP (Constantinides et al., 2011). Additionally, higher concentrations of sevoflurane are known ablate the dysreflexic response to visceral stimulation in human individuals after SCI (Yoo et al., 2008). In future studies, the anesthesia delivery system will be optimized by using a latex membrane to cover the face mask, similar to methods used by Tsukamoto et al., 2015 (Tsukamoto et al., 2015). This intervention should allow for more consistent concentrations of anesthesia inhaled by each mouse and potentially less fluctuations in baseline BP and HR.

4.2.4. Difficulties with ETS

We attempted to use ETS as a novel, non-invasive stimulus modality to induce cardiorespiratory responses in mice. In over half of our experiments, tail stimulation failed to increase the BP, even in animals where foot stimulation resulted in BP increases. One possible explanation is a

combination of crush and ischemic injury to the tail nerves while the electrode clips were attached. The lack of muscle activation was often evident upon the second or later trials (with about 5 min wait times between trials. Removing the electrodes during periods of rest would likely reduce the possibility of such an injury and allow tail stimulation to be used as a pressor stimulus.

The surface of the tail skin is also thicker and dryer than the digits or ankle of the mice. Coupled with the larger distance from the surface electrodes to the tail nerves, there was likely a greater resistance in the current path during tail stimulation. We have not attempted to apply water-based gel to the surface of the electrode contact sites, but they may increase the efficiency of stimulation.

We also have not yet optimized the ideal configuration i.e. the electrode position of negative vs positive leads with respect to the base of the tail, and findings from our current trials suggest that cardiovascular responses may vary with different electrode configurations on the tail in the same animal (data not shown).

Another problem encountered with ETS was that small movements were difficult to detect while identifying the MTH. We attempted to use the microscope to increase visualization of contractions, as this aided greatly during foot stimulation, but small movements could still have been missed.

4.3. The bradycardic response to CRD in isoflurane anaesthetized mice

Our observation of a downward trend in HR to noxious stimulation in mice (Cx36WT/KO) was similar to that of Lall et al., 2017, in which they observed bradycardic responses in Cx36WT and Cx36KO mice during peripheral chemoreceptor stimulation. Despite isoflurane being the

anesthetic in the studies reported by Lall et al. and in our experiment; the magnitude of HR drop was 40 – 90 beats/min on average in the study by Lall et al., compared to 9 – 18 beats/min on average in our experiments. Important differences between these studies are that we used visceral noxious stimulation, while Lall et al. injected 0.03% sodium cyanide systemically. Additionally, while we used cerebrally and spinally intact mice, Lall et al. used decerebrate whole heart brain preparations (Lall et al., 2017).

Previous studies have reported an increase in HR during noxious stimulation in conscious, spinally intact mice (Zhang et al., 2013). The experiments, however, were performed only on female C57BL/6 mice strains, while our current study used both male and female C57BL/6 mice Cx36WT and Cx36KO mice. In spinally intact rats, there is evidence for a bradycardic response to noxious stimulation anaesthetized with alpha-chloralose or pentobarbital (Ness and Gebhart, 1988). However, in these experiments, the BP was also reported to decrease during noxious stimulation.

Although we did not obtain data from spinalized mice, existing literature has shown mixed results in HR changes during noxious stimulation after SCI. Recent work from Jarve et al., 2019 demonstrated a bradycardic response to noxious stimulation in conscious, spinalized mice (Jarve et al., 2019). However, rats have shown both bradycardic and tachycardic responses to bladder distention, one day after spinal cord transection (Krassioukov and Weaver, 1995). Additionally, spinalized rats anaesthetized with alpha chloralose showed small increases in BP and HR during CRD (Chau et al., 2000).

4.4. Opposing blood pressure changes in Cx36WT and Cx36KO mice during CRD

Cx36KO mice are known to have an increased BP following peripheral chemoreceptor activation with sodium cyanide, but this response is attenuated compared to Cx36WT mice (Lall et al., 2017). Here we have shown that there is a reduction in BP during CRD in Cx36KO mice. One possible explanation is the isoflurane mediated suppression of the ANS (Skovsted and Sapthavichaikul, 1977). Perhaps when combined with the expected bradycardic response to CRD, Cx36KO are unable to generate sufficient sympathetic outflow to increase the BP. However, given that Lall et al. used isoflurane in their preparation and observed a BP increase during chemoreceptor activation, we would expect a BP increase in our anesthetized Cx36KO mice as well. Also, the fact that we could increase the BP in the Cx36KO mice using either intra-tracheal epinephrine or EFS suggests that isoflurane induced suppression of the ANS was not the major factor causing a reduction in the BP during CRD.

A study using C57/BL6 mice, the parent strain on which the mutation was introduced, investigated the effects of peripheral chemoreceptor stimulation with intravenous potassium cyanide on BP (Braga et al., 2008). After drug administration, this study described an increase followed by a decrease in BP. This initial increase was completely abolished when the mice were treated by prazosin, that is an α_1-adrenergic antagonist. This suggested to Braga and colleagues, that the initial rapid rise in the BP was resulted from an increase in the sympathetic drive to the vasculature. Based on this previous study, we hypothesize that in our experiments, the BP reduction in the Cx36 KO mice resulted, in part, from an inadequate increase in sympathetic drive to the vasculature. The lack of synchronized drive to the vasculature or the lack of sufficient number of neurons recruited by the CRD response in the mice lacking the Cx36 protein could be a plausible explanation for the lack of the BP increase.

Maybe the longest recognized factor to attenuate BP changes is the blockade of the alpha-1B adrenergic receptors, however this blockade is not known to reverse the pressor response to a BP decrease, e.g. (Cavalli et al., 1997). Another factor known to attenuate BP changes is analgesics, for example, buprenorphine can attenuate pressor responses (Shafford and Schadt, 2008b, Shafford and Schadt, 2008a). Catalase (a peripheral factor) overexpression, attenuated BP increase (when measured by tail-cuff) after NE and angiotensin II administration. This occurred due to reduced H_2O_2 production in the arterial walls of intact mice (Yang et al., 2003). One other factor present in the central nervous system that is known to attenuate BP increases after CRD is blockade of metabotropic glutamate receptor 5 (mGluR5) (Lindstrom et al., 2008). The lack of Cx36 may prevent or delay activation of mGluR5s. Furthermore, transient receptor potential V1 (TRPV1) channels may be also altered due to the lack of Cx36 (Nagy et al., 2018). This was further evidenced by studies investigating the inflammatory response to noxious stimuli in mice. After noxious nociceptive stimulation of the paw and ears, Cx36KO mice showed delayed and attenuated extravasation of circulating Evan's blue dye in male mice (Bhullar, 2017).

A previous study with premammillary–precollicular decerebrate cats compared pharmacologically induced pressor responses to spontaneous motor activity induced pressor responses. There was a simultaneous tachycardia during the pressor response to spontaneous motor activity, while the pressor response during phenylephrine or NE administration elicited a baroreflex bradycardia (Matsukawa et al., 2014). Therefore, the stimulus modality used to evoke a pressor response also influences the cardiovascular response observed – including the direction of BP change. At this point, we are uncertain why Cx36KO mice have a decrease in BP during CRD and more experiments are necessary to verify the statistical differences we report here.

4.5. Future directions

Use of gap junctional blockers in adult, spinally intact Cx36WT mice

In order to estimate the endogenous contribution of Cx36 containing gap junctions in mediating the sympathetic response to noxious stimuli, cardiorespiratory responses to noxious stimuli will be measured before and after administration of gap junction antagonists in neurally-intact and spinal wild-type mice. The antimalarial drug, mefloquine, has proven to be a relatively specific blocker of gap junctions containing Cx36, though mefloquine also has inhibitory effects of Cx40, Cx43 and Cx50 containing gap junctions. However, the effect of mefloquine on different gap junctions appears to have a dose dependent effect (Willebrords et al., 2017).

Mefloquine has also been used in whole heart brain stem preparations of male Wistar rats. After addition of mefloquine to the perfusate, sodium cyanide induced excitation of the lower thoracic sympathetic chain was reduced (Lall et al., 2012). The antimalarial drug mefloquine will therefore be administered to Cx36WT mice, while monitoring cardiorespiratory parameters during noxious stimulation, and comparing the changes in parameters with Cx36KO and Cx36WT administered a saline vehicle.

The role of Cx36 in the development of cardiorespiratory changes after SCI

We intend to use our experimental model in Cx36WT and Cx36KO mice in the subacute period after complete spinal cord transection. Mice have been shown to develop spontaneous and induced episodes of AD within 5 – 14 days after spinal cord transection (Jacob et al., 2003, Jacob et al., 2001, Zhang et al., 2013). Data from our current experiments has shown that both Cx36WT and Cx36KO mice have changes in their RR and pattern during noxious stimulation in the intact state. We learned from the experiments that monitoring the respiratory changes during

CRD and EFS in spinalized mice may also be beneficial, as previous AD rodent models have not reported changes in RR during noxious stimulation. We also learned that introducing a daily testing protocol using tail-cuff BP monitoring (non-invasive) on conscious mice would be possible to be combined with these terminal, single-time point experiments in the future. The changes in the conscious and anesthetized mice likely will be different in magnitude, as it has been the case in rats.

Identifying the functional role of Cx36 in cell-cell communication between SPNs

In future experiments, the functional role of Cx36 in SPNs will be investigated by using dye injection studies. Dye coupling between thoracic SPNs in Cx36KO and Cx36WT mice will be observed using immunofluorescence techniques similar to previous studies (Blivis et al., 2019). Dye transfer between coupled neurons will be observed under microscopy, giving insight into the strength and degree of coupling between neurons. The role of Cx36 in coupling will be investigated by applying mefloquine to the preparations, comparing the extent of dye transfer to preparations exposed to a control such as saline. Dye coupling will also be measured before and after high thoracic SCI to detect functional changes in Cx36 containing gap junctions after SCI.

4.6. Summary of the potential therapeutic capacity of connexins after SCI

This study focused on the putative role of neuron-to-neuron gap junctions (Cx36) in sympatho-excitation. Future studies will evaluate changes in the regulation of Cx36 after SCI in mice, as previous investigators have shown a transient decrease in Cx36 protein levels after SCI in rats (Yates et al., 2008). However, other connexins may contribute to pathophysiological changes after spinal cord injury. In continuity with this project, future experiments will examine changes in other connexins, potentially increasing the translational outcomes of these studies. Some of the known mechanisms by which different connexins alter neural function are the discussed below.

Cx32 and Cx47 are specific to oligodendrocytes, and Schwan cells respectively. Defects in genes that encode the gap junction proteins Cx32 and Cx47 have been implicated in the X linked form of Charcot-Marie-Tooth disease and Pelizaeus-Merzbacher-like disease respectively, which are diseases of demyelination and hypomyelination (Dermietzel and Spray, 2016, Kleopa, 2011). Mice models with a deletion of genes encoding for both Cx32 and Cx47 suffer from severe demyelination and vacuolation, with areas of absent myelin and usually die by six weeks postnatal. There is some evidence to suggest that the degeneration seen in these mice may result from defective buffering of K^+ ions produced during neural activity, as mice lacking the potassium channel Kir4.1 have phenotypic presentations like double knockout Cx32 and Cx47 mice (Dermietzel and Spray, 2016).

Astrocytes are known to have neuroprotective and neuroregenerative functions, such antioxidant release, energy metabolism, immunomodulation, reducing neurotoxicity and angiogenesis (Becerra-Calixto and Cardona-Gomez, 2017). Reactive astrocytes expressing Cx43 migrate towards sites of stab wounds and infarcted regions of the post-ischemic brain. However, the glial

scar formation from reactive astrocytosis is also believed to limit axonal regeneration, promote neurotoxicity and drive inflammation (Becerra-Calixto and Cardona-Gomez, 2017, Dermietzel and Spray, 2016).

A plausible theory is that astrocytes, through gap junctions, allow for the diffusion of glucose and other pro-survival metabolites to the ischemic penumbra, and the removal of toxic substances. The reverse is also theoretically possible, where gap junctions allow for diffusion of toxic metabolites and oxidants from a cell more proximal to the infarct, to a cell more distal in the ischemic penumbra, worsening ischemia and injury (Dermietzel and Spray, 2016). In fact, an increased cerebral infarct size is seen in mice with either truncated or deficient Cx43 expression, post-experimental stroke (Kozoriz et al., 2010, Siushansian et al., 2001). Conversely, amelioration of infarct size has also been reported after administration of gap junction blockers in brain slice preparations (Dermietzel and Spray, 2016). Pharmacological blockade or knockout of Cx36 in mice reduced secondary ischemic neuronal death (Belousov et al., 2017). Besides injury to the central nervous system, connexins may also play a role after injury in the peripheral nervous system.

Cx43 staining within the cerebral cortex increases acutely after facial nerve injury (Laskawi et al., 1997). Cx36 staining is also increased in the superficial laminae of the medullary dorsal horn after chronic constriction injury to the infraorbital nerve (CCI-IoN) in rats. Rats subjected to CCI-IoN develop subsequent mechanical allodynia but interestingly, the allodynia is significantly decreased following relatively selective blockade of Cx36 using intracisternal mefloquine (Ouachikh et al., 2018).

5. Conclusion

Despite the small power and sample size of our experiments, we have demonstrated that isoflurane anesthetized Cx36WT and Cx36KO having diverging BP responses to CRD. Cx36WT mice have an increase in BP but Cx36KO have a decrease in BP during CRD. The same mice, both Cx36WT and Cx36KO, simultaneously with the BP response also have a tendency for a bradycardic response to CRD. Previous studies have shown that bradycardia mainly occurs during a pressor response to different stimuli in mice (see Table 5). Isoflurane anesthetized Cx36KO and Cx36WT mice have a tendency for an increase in respiratory rate during noxious stimulation. EFS at a frequency of 4 Hz evokes a graded BP increase in Cx36WT mice, and that also elicits a BP increase in Cx36KO mice, albeit these were also not statistically significant changes. Our results therefore imply that non-invasive EFS may be another stimulation method for inducing autonomic dysreflexia in mice models. One advantage of EFS is that the grading of the electrical stimulus allows selective activation of large diameter afferents (between 1 – 3x MTH) and a combined large and small fiber activation with intensities > 3XMTH.

Table 5.1. Studies examining the cardiovascular response to different stimuli in mice.

Study	Strain	SCI	Parameter	Outcome		
				Chemoreceptor stimulation	Cutaneous skin pinch	CRD
Jarve et al. 2019	C57BL/6	+	HR			↓
	C57BL/6	+	BP			↑
Lall et al. 2017	Cx36WT/KO	-	SPN activity	↑ ↑		
	Cx36WT/KO	-	SPN activity		↑ ↑	
	Cx36WT/KO	-	HR	↓ ↓		
	Cx36WT/KO	-	BP	↑ ↑		
Zhang et al. 2013	C57BL/6	-	BP		↑	↑
	C57BL/6	-	HR		↑	↑
		+	BP		↑	↑
		+	HR		↓	↓
Webb et al. 2006	C57BL/6	+	BP			↑
Jacob et al. 2003	129Sv	+	BP		↑	↑
	C57BL	+	BP		↑	↑
	Wld^S	+	BP		↑	↑
Jacob et al. 2001	129Sv	+	BP		↑	↑
	129Sv	-	BP		↑	↑

The columns indicate the reference to the published data (study), the mouse strain examined (strain), the presence or absence of the spinal cord injury (SCI), the parameters tested: heart rate (HR), blood pressure (BP), sympathetic nerve recordings (SPN activity), and the change in parameters in response different stimuli (Outcome). Up arrows represent increases, down arrows represent decreases. Blue arrows represent data from Cx36WT; and orange arrows represent data from Cx36KO mice, black arrows show data from other strains.

6. References

ALLEN, K. J. & LESLIE, S. W. 2019. Autonomic Dysreflexia. *StatPearls.* Treasure Island (FL).

ANGELI, C. A., BOAKYE, M., MORTON, R. A., VOGT, J., BENTON, K., CHEN, Y., FERREIRA, C. K. & HARKEMA, S. J. 2018. Recovery of Over-Ground Walking after Chronic Motor Complete Spinal Cord Injury. *N Engl J Med,* 379**,** 1244-1250.

BAUTISTA, W., MCCREA, D. A. & NAGY, J. I. 2014. Connexin36 identified at morphologically mixed chemical/electrical synapses on trigeminal motoneurons and at primary afferent terminals on spinal cord neurons in adult mouse and rat. *Neuroscience,* 263**,** 159-80.

BAUTISTA, W. & NAGY, J. I. 2014. Connexin36 in gap junctions forming electrical synapses between motoneurons in sexually dimorphic motor nuclei in spinal cord of rat and mouse. *Eur J Neurosci,* 39**,** 771-87.

BAUTISTA, W., NAGY, J. I., DAI, Y. & MCCREA, D. A. 2012. Requirement of neuronal connexin36 in pathways mediating presynaptic inhibition of primary afferents in functionally mature mouse spinal cord. *J Physiol,* 590**,** 3821-39.

BECERRA-CALIXTO, A. & CARDONA-GOMEZ, G. P. 2017. The Role of Astrocytes in Neuroprotection after Brain Stroke: Potential in Cell Therapy. *Front Mol Neurosci,* 10**,** 88.

BELOUSOV, A. B., FONTES, J. D., FREITAS-ANDRADE, M. & NAUS, C. C. 2017. Gap junctions and hemichannels: communicating cell death in neurodevelopment and disease. *BMC Cell Biol,* 18**,** 4.

BENNETT, M. V. & ZUKIN, R. S. 2004. Electrical coupling and neuronal synchronization in the Mammalian brain. *Neuron,* 41**,** 495-511.

BENNETT, M. V. L. 1997. Gap junctions as electrical synapses. *Journal of Neurocytology,* 26**,** 349-366.

BENNETT, M. V. L. 2011. Electrical Transmission: A Functional Analysis and Comparison to Chemical Transmission. *Comprehensive Physiology*.

BHULLAR, P. K. 2017. *Role of connexin36 proteins in peripheral nerves during the triple response and pain.* MASTER OF SCIENCE, University of Manitoba.

BLIVIS, D., FALGAIROLLE, M. & O'DONOVAN, M. J. 2019. Dye-coupling between neonatal spinal motoneurons and interneurons revealed by prolonged back-filling of a ventral root with a low molecular weight tracer in the mouse. *Scientific Reports,* 9.

BRAGA, V. A., BURMEISTER, M. A., SHARMA, R. V. & DAVISSON, R. L. 2008. Cardiovascular responses to peripheral chemoreflex activation and comparison of different methods to evaluate baroreflex gain in conscious mice using telemetry. *Am J Physiol Regul Integr Comp Physiol,* 295**,** R1168-74.

BRODAL, P. 2016. *The central nervous system*.

CABOT, J. B. 1990. Sympathetic Preganglionic Neurons: Cytoarchitecture, infrastructure, and Biophysical Properties. *In:* LOEWY, A. D. & SPYER, K. M. (eds.) *Central Regulation of Autonomic Functions.* New York: Oxford University Press.

CAVALLI, A., LATTION, A. L., HUMMLER, E., NENNIGER, M., PEDRAZZINI, T., AUBERT, J. F., MICHEL, M. C., YANG, M., LEMBO, G., VECCHIONE, C., MOSTARDINI, M., SCHMIDT, A., BEERMANN, F. & COTECCHIA, S. 1997. Decreased blood pressure response in mice deficient of the alpha1b-adrenergic receptor. *Proc Natl Acad Sci U S A,* 94**,** 11589-94.

CENTER, N. S. C. I. S. 2019. Spinal Cord Injury Facts and Figures at a Glance. *In:* CENTER, N. S. C. I. S. (ed.). Birmingham, AL: University of Alabama at Birmingham.

CHAU, D., JOHNS, D. G. & SCHRAMM, L. P. 2000. Ongoing and stimulus-evoked activity of sympathetically correlated neurons in the intermediate zone and dorsal horn of acutely spinalized rats. *Journal of neurophysiology,* 83**,** 2699-707.

CHOPRA, A. S., MIYATANI, M. & CRAVEN, B. C. 2018. Cardiovascular disease risk in individuals with chronic spinal cord injury: Prevalence of untreated risk factors and poor adherence to treatment guidelines. *J Spinal Cord Med,* 41**,** 2-9.

CLARKE, J. L. 1859. Further researches on the gray siihstance of the spinal cord. *Philosophical Transactions of the Royal Society of London,* 149.

CLARKE, J. L. & SAMUELS, S. 1851. Researches into the structure of the spinal chord. *Philosophical Transactions of the Royal Society of London,* 141**,** 607-608.

CONDORELLI, D. F., PARENTI, R., SPINELLA, F., TROVATO SALINARO, A., BELLUARDO, N., CARDILE, V. & CICIRATA, F. 1998. Cloning of a new gap junction gene (Cx36) highly expressed in mammalian brain neurons. *Eur J Neurosci,* 10**,** 1202-8.

CONSTANTINIDES, C., MEAN, R. & JANSSEN, B. J. 2011. Effects of isoflurane anesthesia on the cardiovascular function of the C57BL/6 mouse. *ILAR J,* 52**,** e21-31.

CONTA, A. C. & STELZNER, D. J. 2009. The Propriospinal Network. *In:* WATSON, C., PAXINOS, G. & KAYALIOGLU, G. (eds.) *The spinal cord a Christopher and Dana Reeve Foundation text and atlas.* 1st ed. Amsterdam ; Boston: Elsevier/Academic Press.

COWLEY, K. C., ZAPOROZHETS, E. & SCHMIDT, B. J. 2010. Propriospinal transmission of the locomotor command signal in the neonatal rat. *Ann N Y Acad Sci,* 1198**,** 42-53.

CURTI, S., HOGE, G., NAGY, J. I. & PEREDA, A. E. 2012. Synergy between electrical coupling and membrane properties promotes strong synchronization of neurons of the mesencephalic trigeminal nucleus. *J Neurosci,* 32**,** 4341-59.

DERE, E. & ZLOMUZICA, A. 2012. The role of gap junctions in the brain in health and disease. *Neurosci Biobehav Rev,* 36**,** 206-17.

DERMIETZEL, R. & SPRAY, D. C. 2016. Gap Junctions and Electric Synapses. *In:* PFAFF, D. W. & VOLKOW, N. D. (eds.) *Neuroscience in the 21st Century: From Basic to Clinical.* New York, NY: Springer New York.

DEUCHARS, S. A. & LALL, V. K. 2015. Sympathetic preganglionic neurons: properties and inputs. *Compr Physiol,* 5**,** 829-69.

ELDAHAN, K. C. & RABCHEVSKY, A. G. 2018. Autonomic dysreflexia after spinal cord injury: Systemic pathophysiology and methods of management.

FRISCH, C., DE SOUZA-SILVA, M. A., SOHL, G., GULDENAGEL, M., WILLECKE, K., HUSTON, J. P. & DERE, E. 2005. Stimulus complexity dependent memory impairment and changes in motor performance after deletion of the neuronal gap junction protein connexin36 in mice. *Behav Brain Res,* 157**,** 177-85.

FROSTELL, A., HAKIM, R., THELIN, E. P., MATTSSON, P. & SVENSSON, M. 2016. A Review of the Segmental Diameter of the Healthy Human Spinal Cord. *Front Neurol,* 7**,** 238.

FURSHPAN, E. J. & POTTER, D. D. 1959. Transmission at the giant motor synapses of the crayfish. *J Physiol,* 145**,** 289-325.

GALARRETA, M. & HESTRIN, S. 1999. A network of fast-spiking cells in the neocortex connected by electrical synapses. *Nature,* 402**,** 72-5.

GONZALEZ, H. L., CARMICHAEL, N., DOSTROVSKY, J. O. & CHARLTON, M. P. 2005. Evaluation of the time course of plasma extravasation in the skin by digital image analysis. *J Pain,* 6**,** 681-8.

HARRISON, M., O'BRIEN, A., ADAMS, L., COWIN, G., RUITENBERG, M. J., SENGUL, G. & WATSON, C. 2013. Vertebral landmarks for the identification of spinal cord segments in the mouse. *Neuroimage,* 68**,** 22-9.

HEISE, C. & KAYALIOGLU, G. 2009. Spinal Cord Transmitter Substances. *In:* WATSON, C., PAXINOS, G. & KAYALIOGLU, G. (eds.) *The spinal cord a Christopher and Dana Reeve Foundation text and atlas.* 1st ed. Amsterdam ; Boston: Elsevier/Academic Press.

HOU, S. & RABCHEVSKY, A. G. 2014. Autonomic consequences of spinal cord injury. *Comprehensive Physiology*.

JACOB, J. E., GRIS, P., FEHLINGS, M. G., WEAVER, L. C. & BROWN, A. 2003. Autonomic dysreflexia after spinal cord transection or compression in 129Sv, C57BL, and Wallerian degeneration slow mutant mice. *Experimental Neurology,* 183**,** 136-146.

JACOB, J. E., PNIAK, A., WEAVER, L. C. & BROWN, A. 2001. Autonomic dysreflexia in a mouse model of spinal cord injury. *Neuroscience,* 108**,** 687-693.

JACOBSON, G. M., VOSS, L. J., MELIN, S. M., MASON, J. P., CURSONS, R. T., STEYN-ROSS, D. A., STEYN-ROSS, M. L. & SLEIGH, J. W. 2010. Connexin36 knockout mice display increased sensitivity to pentylenetetrazol-induced seizure-like behaviors. *Brain Res,* 1360**,** 198-204.

JARVE, A., TODIRAS, M., LIAN, X., FILIPPELLI-SILVA, R., QADRI, F., MARTIN, R. P., GOLLASCH, M. & BADER, M. 2019. Distinct roles of angiotensin receptors in

autonomic dysreflexia following high-level spinal cord injury in mice. *Exp Neurol,* 311**,** 173-181.

KATSUMARU, H., KOSAKA, T., HEIZMANN, C. W. & HAMA, K. 1988. Gap junctions on GABAergic neurons containing the calcium-binding protein parvalbumin in the rat hippocampus (CA1 region). *Exp Brain Res,* 72**,** 363-70.

KAYALIOGLU, G. 2009. The Vertebral Column and Spinal Meninges. *In:* WATSON, C., PAXINOS, G. & KAYALIOGLU, G. (eds.) *The spinal cord a Christopher and Dana Reeve Foundation text and atlas.* 1st ed. Amsterdam ; Boston: Elsevier/Academic Press.

KIRKCALDIE, M. T. K. 2012. Neocortex. *In:* WATSON, C., PAXINOS, G. & PUELLES, L. (eds.) *The mouse nervous system.* 1st ed. Amsterdam: Elsevier/Academic Press.

KLEOPA, K. A. 2011. The role of gap junctions in Charcot-Marie-Tooth disease. *J Neurosci,* 31**,** 17753-60.

KOSEOGLU, B. F., SAFER, V. B., OKEN, O. & AKSELIM, S. 2017. Cardiovascular disease risk in people with spinal cord injury: is there a possible association between reduced lung function and increased risk of diabetes and hypertension? *Spinal Cord,* 55**,** 87-93.

KOZORIZ, M. G., BECHBERGER, J. F., BECHBERGER, G. R., SUEN, M. W., MORENO, A. P., MAASS, K., WILLECKE, K. & NAUS, C. C. 2010. The connexin43 C-terminal region mediates neuroprotection during stroke. *J Neuropathol Exp Neurol,* 69**,** 196-206.

KRASSIOUKOV, A., WARBURTON, D. E., TEASELL, R., ENG, J. J. & SPINAL CORD INJURY REHABILITATION EVIDENCE RESEARCH, T. 2009. A systematic review of the management of autonomic dysreflexia after spinal cord injury. *Arch Phys Med Rehabil,* 90**,** 682-95.

KRASSIOUKOV, A. V. & WEAVER, L. C. 1995. Reflex and morphological changes in spinal preganglionic neurons after cord injury in rats. *Clinical and Experimental Hypertension,* 17**,** 361-373.

LALL, V. K., BRUCE, G., VOYTENKO, L., DRINKHILL, M., WELLERSHAUS, K., WILLECKE, K., DEUCHARS, J. & DEUCHARS, S. A. 2017. Physiologic regulation of heart rate and blood pressure involves connexin 36-containing gap junctions. *FASEB J,* 31**,** 3966-3977.

LALL, V. K., DUTSCHMANN, M., DEUCHARS, J. & DEUCHARS, S. A. 2012. The anti-malarial drug Mefloquine disrupts central autonomic and respiratory control in the working heart brainstem preparation of the rat. *J Biomed Sci,* 19**,** 103.

LASKAWI, R., ROHLMANN, A., LANDGREBE, M. & WOLFF, J. R. 1997. Rapid astroglial reactions in the motor cortex of adult rats following peripheral facial nerve lesions. *Eur Arch Otorhinolaryngol,* 254**,** 81-5.

LEE, E. S. & JOO, M. C. 2017. Prevalence of Autonomic Dysreflexia in Patients with Spinal Cord Injury above T6. *Biomed Res Int,* 2017**,** 2027594.

LINDSTROM, E., BRUSBERG, M., HUGHES, P. A., MARTIN, C. M., BRIERLEY, S. M., PHILLIS, B. D., MARTINSSON, R., ABRAHAMSSON, C., LARSSON, H., MARTINEZ, V. & BLACKSHAW, L. A. 2008. Involvement of metabotropic glutamate 5 receptor in visceral pain. *Pain,* 137**,** 295-305.

MARINA, N., BECKER, D. L. & GILBEY, M. P. 2008. Immunohistochemical detection of connexin36 in sympathetic preganglionic and somatic motoneurons in the adult rat. *Auton Neurosci,* 139**,** 15-23.

MATSUKAWA, K., ISHII, K., KADOWAKI, A., ISHIDA, T., IDESAKO, M. & LIANG, N. 2014. Discharges of aortic and carotid sinus baroreceptors during spontaneous motor activity and pharmacologically evoked pressor interventions. *J Physiol Sci,* 64**,** 291-303.

MCCORRY, L. K. 2007. Physiology of the autonomic nervous system. *Am J Pharm Educ,* 71**,** 78.

NAGY, J. I. 2012. Evidence for connexin36 localization at hippocampal mossy fiber terminals suggesting mixed chemical/electrical transmission by granule cells. *Brain Res,* 1487**,** 107-22.

NAGY, J. I., BAUTISTA, W., BLAKLEY, B. & RASH, J. E. 2013. Morphologically mixed chemical-electrical synapses formed by primary afferents in rodent vestibular nuclei as revealed by immunofluorescence detection of connexin36 and vesicular glutamate transporter-1. *Neuroscience,* 252**,** 468-88.

NAGY, J. I., LYNN, B. D., SENECAL, J. M. M. & STECINA, K. 2018. Connexin36 Expression in Primary Afferent Neurons in Relation to the Axon Reflex and Modality Coding of Somatic Sensation. *Neuroscience,* 383**,** 216-234.

NAGY, J. I. & RASH, J. E. 2000. Connexins and gap junctions of astrocytes and oligodendrocytes in the CNS. *Brain Res Brain Res Rev,* 32**,** 29-44.

NAGY, J. I., URENA-RAMIREZ, V. & GHIA, J. E. 2014. Functional alterations in gut contractility after connexin36 ablation and evidence for gap junctions forming electrical synapses between nitrergic enteric neurons. *FEBS Lett,* 588**,** 1480-90.

NAKAMURA, Y., MORIOKA, N., ZHANG, F. F., HISAOKA-NAKASHIMA, K. & NAKATA, Y. 2015. Downregulation of connexin36 in mouse spinal dorsal horn neurons leads to mechanical allodynia. *J Neurosci Res,* 93**,** 584-91.

NESS, T. J. & GEBHART, G. F. 1988. Colorectal distension as a noxious visceral stimulus: physiologic and pharmacologic characterization of pseudaffective reflexes in the rat. *Brain Research,* 450**,** 153-169.

NICHOLLS, J. G. & PURVES, D. 1972. A comparison of chemical and electrical synaptic transmission between single sensory cells and a motoneurone in the central nervous system of the leech. *J Physiol,* 225**,** 637-56.

NIELSEN, M. S., AXELSEN, L. N., SORGEN, P. L., VERMA, V., DELMAR, M. & HOLSTEIN-RATHLOU, N. H. 2012. Gap junctions. *Compr Physiol,* 2**,** 1981-2035.

NOLAN, M. F., LOGAN, S. D. & SPANSWICK, D. 1999. Electrophysiological properties of electrical synapses between rat sympathetic preganglionic neurones in vitro. *J Physiol,* 519 Pt 3**,** 753-64.

NOONAN, V. K., FINGAS, M., FARRY, A., BAXTER, D., SINGH, A., FEHLINGS, M. G. & DVORAK, M. F. 2012. Incidence and Prevalence of Spinal Cord Injury in Canada: A National Perspective. *Neuroepidemiology,* 38**,** 219-226.

OUACHIKH, O., HAFIDI, A., BOUCHER, Y. & DIEB, W. 2018. Electrical Synapses are Involved in Orofacial Neuropathic Pain. *Neuroscience,* 382**,** 69-79.

RABCHEVSKY, A. G. 2006. Segmental organization of spinal reflexes mediating autonomic dysreflexia after spinal cord injury. *Prog Brain Res,* 152**,** 265-74.

REXED, B. 1952. The cytoarchitectonic organization of the spinal cord in the cat. *J Comp Neurol,* 96**,** 414-95.

SAHA, U. & JAYALAKSHMI, T. 2003. Pressor response and hypertension. *Indian Journal of Anaesthesia,* 47**,** 442-442.

SAVIC, G., DEVIVO, M. J., FRANKEL, H. L., JAMOUS, M. A., SONI, B. M. & CHARLIFUE, S. 2017. Long-term survival after traumatic spinal cord injury: a 70-year British study. *Spinal Cord,* 55**,** 651-658.

SENGUL, G. & WATSON, C. 2012. Spinal Cord. *In:* WATSON, C., PAXINOS, G. & PUELLES, L. (eds.) *The mouse nervous system.* 1st ed. Amsterdam: Elsevier/Academic Press.

SHAFFORD, H. L. & SCHADT, J. C. 2008a. Effect of buprenorphine on the cardiovascular and respiratory response to visceral pain in conscious rabbits. *Vet Anaesth Analg,* 35**,** 333-40.

SHAFFORD, H. L. & SCHADT, J. C. 2008b. Respiratory and cardiovascular effects of buprenorphine in conscious rabbits. *Vet Anaesth Analg,* 35**,** 326-32.

SHARIF, H. & HOU, S. 2017. Autonomic dysreflexia: a cardiovascular disorder following spinal cord injury. *Neural Regen Res,* 12**,** 1390-1400.

SIUSHANSIAN, R., BECHBERGER, J. F., CECHETTO, D. F., HACHINSKI, V. C. & NAUS, C. C. 2001. Connexin43 null mutation increases infarct size after stroke. *J Comp Neurol,* 440**,** 387-94.

SKOVSTED, P. & SAPTHAVICHAIKUL, S. 1977. The effects of isoflurane on arterial pressure, pulse rate, autonomic nervous activity, and barostatic reflexes. *Can Anaesth Soc J,* 24**,** 304-14.

SOHL, G., DEGEN, J., TEUBNER, B. & WILLECKE, K. 1998. The murine gap junction gene connexin36 is highly expressed in mouse retina and regulated during brain development. *FEBS Lett,* 428**,** 27-31.

SQUAIR, J. W., PHILLIPS, A. A., HARMON, M. & KRASSIOUKOV, A. V. 2016. Emergency management of autonomic dysreflexia with neurologic complications. *CMAJ,* 188**,** 1100-1103.

SUNDARAM, K., MURUGAIAN, J. & SAPRU, H. 1989. Cardiac responses to the microinjections of excitatory amino acids into the intermediolateral cell column of the rat spinal cord. *Brain Res,* 482**,** 12-22.

TSUKAMOTO, A., SERIZAWA, K., SATO, R., YAMAZAKI, J. & INOMATA, T. 2015. Vital signs monitoring during injectable and inhalant anesthesia in mice. *Exp Anim,* 64**,** 57-64.

UENO, M., UENO-NAKAMURA, Y., NIEHAUS, J., POPOVICH, P. G. & YOSHIDA, Y. 2016. Silencing spinal interneurons inhibits immune suppressive autonomic reflexes caused by spinal cord injury. *Nature Neuroscience*.

WAN, D. & KRASSIOUKOV, A. V. 2014. Life-threatening outcomes associated with autonomic dysreflexia: a clinical review. *J Spinal Cord Med,* 37**,** 2-10.

WAXMAN, S. G. 2017. The Autonomic Nervous System. *Clinical Neuroanatomy, 28e.* New York, NY: McGraw-Hill Education.

WEBB, A. A., CHAN, C. B., BROWN, A. & SALEH, T. M. 2006. Estrogen reduces the severity of autonomic dysfunction in spinal cord-injured male mice. *Behavioural Brain Research,* 171**,** 338-349.

WEHRWEIN, E. A., ORER, H. S. & BARMAN, S. M. 2016. Overview of the Anatomy, Physiology, and Pharmacology of the Autonomic Nervous System. *Compr Physiol,* 6**,** 1239-78.

WILLEBRORDS, J., MAES, M., CRESPO YANGUAS, S. & VINKEN, M. 2017. Inhibitors of connexin and pannexin channels as potential therapeutics. *Pharmacol Ther,* 180**,** 144-160.

YANG, H., SHI, M., VANREMMEN, H., CHEN, X., VIJG, J., RICHARDSON, A. & GUO, Z. 2003. Reduction of pressor response to vasoconstrictor agents by overexpression of catalase in mice. *Am J Hypertens,* 16**,** 1-5.

YATES, C., CHARLESWORTH, A., ALLEN, S. R., REESE, N. B., SKINNER, R. D. & GARCIA-RILL, E. 2008. The onset of hyperreflexia in the rat following complete spinal cord transection. *Spinal Cord,* 46**,** 798-803.

YOO, K. Y., JEONG, C. W., KIM, S. J., CHUNG, S. T., BAE, H. B., OH, K. J. & LEE, J. 2008. Sevoflurane concentrations required to block autonomic hyperreflexia during transurethral litholapaxy in patients with complete spinal cord injury. *Anesthesiology,* 108**,** 858-63.

ZHANG, Y., GUAN, Z., READER, B., SHAWLER, T., MANDREKAR-COLUCCI, S., HUANG, K., WEIL, Z., BRATASZ, A., WELLS, J., POWELL, N. D., SHERIDAN, J. F., WHITACRE, C. C., RABCHEVSKY, A. G., NASH, M. S. & POPOVICH, P. G. 2013. Autonomic Dysreflexia Causes Chronic Immune Suppression after Spinal Cord Injury. *Journal of Neuroscience,* 33**,** 12970-12981.